Evaluation of ROS production in OXPHOS knockout strains of C. elegans

C Dreyer

orcid.org 0000-0002-5217-1157

Dissertation accepted in partial fulfilment of the requirements for the degree *Master of Science in Biochemistry* at the North-West University

Supervisor: Prof FH van der Westhuizen

Co-supervisor: Dr CF Labuschagne

Graduation May 2024

25055798

ACKNOWLEDGEMENTS

First and foremost, I extend my heartfelt gratitude to **God** for granting me the strength, guidance, and perseverance throughout this dissertation journey, enabling its completion.

To my study leader, **Prof Francois**, most definitely the best supervisor, mentor, and confidant. Thank you for the atmosphere you have cultivated in the Mitochondria Research Laboratory, it is truly exceptional and something I will always hold dear. Your invaluable contributions have made my thesis a reality, and I am profoundly grateful for your support, patience, humour and guidance throughout this journey and thank you for the pro golf tips and days.
To **Dr. Stiaan**, thank you for assisting during endless times during the microscope sessions. Thank you for your guidance and support.

I would like to thank the following people who contributed to the completion of this dissertation:

- The **NWU** for financial support.
- To the **National Research Foundation (NRF)** towards this research is hereby acknowledged.
- **Dr Maryke Schoonen** for her assistance in genotyping, data processing and editing.
- **Prof Chrisna Gouws** and **Anja Haasbroek-Pheiffer** for their assistance with the Zeiss Microscopy analyses.
- **Dr Gerhard du Preez** for training and the set up for *C. elegans*.
- **Valerie Viljoen** for her fast and flawless assistance in language and grammatical editing.
- To all the **colleagues at the Mito lab** for their support, laughs and fun times.

To my mother, **Sharon**, father, **Pierre**, sister, **Antoinette,** and brother **Juan** for all the motivation, love, and support throughout the years. Without whom none of this would be possible.
To my dearest friend, **Bernize**, for all the support, encouragement, and your understanding. You have been my rock throughout this study.
To all my **friends,** for their support, endless questioning on what I am doing and for their motivation.

ABSTRACT

The oxidative phosphorylation (OXPHOS) system, comprising five complexes, regulates electron transport and adenosine triphosphate (ATP) synthesis in mitochondria. Dysfunctions in these complexes lead to diverse diseases. Reactive oxygen species (ROS), as by-products of OXPHOS, contribute to cellular regulation but also stress, potentially causing oxidative damage and disease.

Investigating ROS-associated diseases requires robust model systems. Caenorhabditis elegans (*C. elegans*), due to its genetic manipulability and conserved mitochondrial functions, offers a promising platform. This study focuses on primary mitochondrial diseases, particularly deficiencies in OXPHOS, using *C. elegans* as an *in vivo* model to explore ROS formation and potential therapeutic interventions. Current research highlights the need for well-characterised models to study ROS in mitochondrial diseases especially *in vivo*. The study aimed to evaluate and elucidate the relationship between OXPHOS dysfunction and mitochondrial ROS in various *C. elegans* strains. Investigations using suitable models are crucial to advance our understanding of ROS-mediated pathologies and therapeutic strategies. Previous mouse models were used to investigate complex I knock out (KO), but experimental analyses are very time consuming, expensive and lacked conclusive evidence of ROS generation and oxidative stress markers.

Therefore, the aim of this study was the evaluation of ROS production in a selected number of OXPHOS KO stains of *C. elegans*. This involved thoroughly researching and identifying commercially available *C. elegans* strains with pathogenic variants in subunits of OXPHOS complexes. After acquiring these strains, which consisted of three for complex I (MQ1333, CW152 and LB25), one for complex II (TK22) and one for complex III (MQ887), as well as the wild type N2 strain and a putative ROS forming superoxide dismutase (SOD) knockout strain (GA184), the methods to maintain nematodes for research purposes were set up and their genotypes confirmed.

The last objective was to evaluate and compare the functional effects of the gene knockdowns using high resolution respirometry, locomotor activity and finally ROS production, respectively. For all the OXPHOS KO strains, except LB25 in respiration, there was a reduction in functionality of these phenotypic parameters. In line with other models of OXPHOS dysfunction, the strains showed significant variability between these parameters, with no clear pattern emerging. Considering the aim of this study, the complex I KO strain, CW152 was identified as the highest ROS-producing strain. These results provide a valuable comparison of functional effects related to OXPHOS dysfunction in five selected *C. elegans* strains. It could provide a springboard for

future investigations, particularly related to ROS production, on mitochondrial disease and therapeutic interventions.

Key terms: oxidative phosphorylation, adenosine triphosphate, electron transport chain, reactive oxygen species, Caenorhabditis elegans, mitochondrial diseases, strains, knockout, oxidative stress, mitochondrial dysfunction, Oroboros Oxygraph 2k

TABLE OF CONTENTS

LIST OF TABLES

LIST OF FIGURES

ABBREVIATIONS

[ ]	Concentration
~	Approximately
°C	Degrees Celsius
$^1O2$	Singlet oxygen
3’	3’-end of the polynucleotide chain
5’ to 3’	Polynucleotide directionality; from the 5’-end to the 3’-end
5’	5’-end of the polynucleotide chain
µg	Microgram
µL	Microlitre
µm	Micrometre
µM	Micromolar
A	
ADP	Adenosine diphosphate
ATP	Adenosine triphosphate
B	
bp	Base pair
C	
$CaCl_2$	Calcium chloride
CAT	Catalogue number
C. elegans	Caenorhabditis elegans

Cd	Cadmium
CGC	Caenorhabditis Genetics Center
CI	Complex I: NADH:ubiquinone oxidoreductase
CII	Complex II: succinate: ubiquinone oxidoreductase
CII	Complex III: ubiquinol:ferrcytochrome c oxidoreductase
CIV	Complex IV: ferrocytochrome-c: oxygen oxidoreductase
CO_2	Carbon dioxide
CoQ	Coenzyme Q
CT	Threshold cycle
Cu	Copper
$CuSO_4.5H_2O$	Copper (II) sulphate pentahydrate
CV	Coefficient of variance
Cyt c	Cytochrome C

D

DAFF	Department of agriculture, forestry, and fisheries
DNA	Deoxyribonucleic acid
dNTP	deoxyribonucleotide triphosphate
dsDNA	Double-stranded deoxyribonucleic acid
dsRNA	Double-stranded ribonucleic acid

E

E. coli	Escherichia coli

EtBr	Ethidium bromide
et al.	et alii (Latin): and others

F

FAD^+	Flavin adenine dinucleotide
$FADH_2$	Reduced flavin adenine dinucleotide
Fwd	Forward

G

g	Gram
GPx	Glutathione peroxidase
GSH	Reduced glutathione

H

H^+	Hydrogen ion; proton
HCl	Hydrogen chloride
H_2O	Water
H_2O_2	Hydrogen peroxide

I

IMM	Inner mitochondrial membrane
IMS	Inner mitochondrial space
in vitro	(Latin): in the glass; (of a process): performed or taking place outside a living organism
in vivo	(Latin): in life; (of any biological process, reaction, or experiment): occurring or made to occur within a living organism

K

K_2HPO_4	di-potassium hydrogen phosphate
KH_2PO_4	Potassium phosphate monobasic
KO	Knockout

L

L	Litre
LB	Luria broth
Ltd	Limited

M

MD	Mitochondrial disease.
MELAS	Mitochondrial encephalomyopathy, lactic acidosis, and stroke-like episodes
$MgSO_4$	Magnesium sulphate
min	Minute(s)
mL	Millilitre
mm	Millimetre
mM	Millimolar
mRNA	Messenger ribonucleic acid
MT	Metallothionein
mtDNA	Mitochondrial DNA

N

n	Number of samples or replicates analysed
NaCl	Sodium chloride
NAD	Nicotinamide adenine dinucleotide
NAD+	Oxidised nicotinamide adenine dinucleotide
NADH	Reduced nicotinamide adenine dinucleotide
NADP+	Oxidised nicotinamide adenine dinucleotide phosphate
NADPH	Reduced nicotinamide adenine dinucleotide phosphate
NaOH	Sodium hydroxide
nDNA	Nuclear DNA
Ndufs4 mouse	Ndufs4 knockout mouse
NWU	North-West University
O	
O_2	Oxygen
O_2^-	Superoxide anion radical
OCR	Oxygen consumption rate
OXPHOS	Oxidative phosphorylation
P	
PCR	Polymerase chain reaction
PDH	Pyruvate dehydrogenase
pmol	Picomole
p-value	Significance value

R

RNA	Ribonucleic acid
ROS	Reactive oxygen species
rpm	Revolutions per minute

S

s	Second(s)
SD	Standard deviation
SOD	Superoxide dismutase
SOP	Standard operating procedure

T

TCA cycle	Tricarboxylic acid cycle

U

UQCRC2	Ubiquinol-cytochrome c reductase core protein II
UV	Ultraviolet

V

V	Volt
v	Version
v/v	Volume (of solute) per volume (of solvent)

W

w/v	Weight (of solute) per weight (of solvent)
WT	Wild type; genetically unaltered sample (specific to this study)

CHAPTER 1 INTRODUCTION

The study of the aging process receives a lot of scientific and public attention as it is of major relevance to general health and disease. One of the leading theories as to why cells age is the "Free Radical Theory of Aging," where the role of bioenergetics is a key element. It is well recognised that mitochondria play an important role in ageing and diseases (Chinnery and Schon, 2003; Knoefler, 2012). Mitochondria are small cytoplasmic organelles surrounded by a double membrane that plays a crucial role in life. They are often called the powerhouses of the cell and provide the energy for regular cell function (Siekevitz, 1957). This is done through a process called oxidative phosphorylation (OXPHOS), where oxygen, glucose and other nutrients are used to generate adenosine triphosphate (ATP) – the energy currency of the cell (Siekevitz, 1957). OXPHOS uses the electron transport chain located on the mitochondrial inner membrane to generate energy for ATP production (Maglioni & Ventura, 2016; Siekevitz, 1957).

The OXPHOS system collectively consists of five complexes (I-V). Complex I (NADH dehydrogenase) is the major entry point for electrons carried by (nicotinamide adenine dinucleotide) NADH, whereas complex II (succinate dehydrogenase) is a second entry point for electrons carried by (flavin adenine dinucleotide) $FADH^2$ and couples the tricarboxylic acid cycle (TCA) and fatty acid oxidation to the respiratory chain. Complex III (cytochrome c reductase) is a compact electron transporter and complex IV (cytochrome c oxidase) catalyses electron transfer to oxygen to eventually produce water. Electrons are carried from one electron transporter to another, which enables the pumping of protons from the mitochondrial matrix into the mitochondrial inner membrane space. This causes a proton gradient generating electrochemical energy that is used by complex V to produce ATP through phosphorylation of ADP (Alberts, 2002). Defects in any of these complexes or subunits may result in a variety of diseases with different phenotypes (Dudkina *et al.*, 2010).

Organisms in an aerobic environment are exposed to reactive oxygen species (ROS), which are formed through normal metabolic processes as well as environmental stresses; for example, cigarette smoke, air pollution and ultraviolet radiation. This stress can make alterations to the physiological activity of cells (Falk *et al.*, 2008; Hu *et al.*, 2018; Van Breusegem *et al.*, 1999). In the mitochondrion, ROS are produced as a by-product of the ETC reactions from leaking electrons causing one-electron reduction of molecular oxygen to form a superoxide anion (Denzel *et al.*, 2019). If there is not a sufficient and successful removal of most of the ROS, an imbalance between ROS synthesis and the removal thereof, can cause what is generally called "oxidative stress" (Back *et al.*, 2012). Thus, the cellular stress defence mechanism plays an important role

in the removal of ROS (Balaban *et al.*, 2005). Overproduction of ROS can lead to oxidative damage of lipids, proteins, and DNA, which can, in turn, contribute to the development of aging and other diseases. To investigate how ROS may lead to different diseases and how the stress affects cells, a good model system is needed to study the processes involved. Even though excessive ROS can cause oxidative damage and a decrease in functional productivity of several cellular processes (Back *et al.*, 2012), ROS may also play an important role in signalling responses (Miranda-Vizuete & Veal, 2017). Indeed, some ROS are needed to trigger cell signalling, while excessive amounts might contribute to mitochondrial dysfunction and/or aging. Miquel and Fleming (1980) formulated the "oxygen radical-mitochondrial injury hypothesis of aging", suggesting that mitochondria are one of the main targets of radical damage (Tzameli, 2012).

We know that the mitochondria and its functions are essential in life, but studying the diseases and defects associated with mitochondria and ROS are very challenging. To address these challenges, model systems such as mice and yeast models were established to study diseases (Ruzzenente, 2016). In 1965, the South African born biologist Sydney Brenner pioneered the soil nematode *Caenorhabditis elegans* (*C. elegans*) as a model system for experiments in diverse areas of biological research (Brenner, 1974). *C. elegans* is a small, microscopic, free-living roundworm with several advantages related to this study. They are easy to culture with a rapid life cycle (3-6 days depending on the temperature) and mainly exist as a self-fertilizing hermaphrodite. They are transparent, making them favourable systems for using fluorescent markers. Genetic manipulation is also easily achieved and many mutant strains are available (Corsi, 2006; Riddle, 1997).

The use of model organisms has led scientists to greatly advance our understanding of many biological processes. To investigate the role of ROS and dysfunction of the OXPHOS system, *in vivo* model systems are essential. *C. elegans* has made such investigations convenient and a great number of genetic models, including OXPHOS, are available and characterized. Another important advantage is that the *C. elegans* mitochondrial functional processes are highly preserved, making gene knockout (KO) strains of *C. elegans* that lack certain components of the OXPHOS system potentially valuable models to study the role of ROS in cellular physiology, aging, and disease. *C. elegans* is, therefore, recognized as a very useful biological model for studying energy-related processes, such as aging, and the connection with the mitochondrion (Gruber *et al.*, 2015).

For this study, the focus will be on genetic deficiencies of the OXPHOS system, which result in what is known as "primary mitochondrial disease", and on *in vivo* models to investigate the cell

biological consequences and responses to such deficiencies. It has been recognised that the investigation of just one of these cell biological consequences, i.e. ROS and adaptive responses to it, has been difficult in more advanced models such as mice (Miller *et al*., 2021).

While Lindeque *et al*. (2010) assessed the involvement of metallothionine (MT) in mitochondrial function and disease, another recent study has shown that *in vivo* MT does not protect against the effects of ROS and, most interestingly, found that the CI-deficient model (Ndufs4 knock out mouse), did not show any clear markers of oxidative stress (Miller *et al*., 2021). This was significant because Ndufs4 KO-deficiency has previously shown an increase in oxidative stress. CI's main function is to transfer electrons from NADH to ubiquinone and is important because if this process doesn't take place, cellular superoxide production can be increased (Distelmaier *et al.*, 2009; Duchen, 2004).

This study concluded that more extensive and tissue-specific ROS analyses are needed, as well as a better model to investigate the mechanisms underlying disease pathology (Miller *et al*., 2021). The availability of *in vivo* mitochondrial disease models are limited and for effectively exploring this potential (Lindeque *et al*., 2010). *C. elegans* provides an alternative option for such investigations and this study will focus on the use of this *in vivo* model to investigate ROS production. Potential models are required to further study adaptive responses, such as MT induction and protection against oxidative stress. As the ROS scavenging capabilities of MT are still unclear *in vivo*, the question remains if MT over-expression influences ROS in such OXHOS-deficient disease models? According to Miller *et al.* (2021), using more appropriate mitochondrial dysfunctional models that show more clearly defined oxidative stress, are needed to better elucidate the potential role of MT and other therapeutic interventions that target the altered redox state of mitochondrial dysfunction.

1.2 Structure of dissertation

This dissertation is presented in five chapters. Chapter 1 provides the background and introduction of the study. Chapter 2 gives a detailed overview of the mitochondria, the OXPHOS system and *C. elegans* as a model for mitochondrial dysfunction. The problem statement, aims and objectives, and an experimental strategy is also given in this chapter. Chapter 3 gives a detailed description of the materials, methods and instrumentations used according to the objectives. Chapter 4 describes the results of this study, and lastly, Chapter 5 provides a short summary of the study's results and the main conclusions that were reached, limitations, as well as the future prospects.

CHAPTER 2 LITERATURE AND PROBLEM STATEMENT

2.1 INTRODUCTION

In this chapter, a brief overview will be given of the mitochondrion, OXPHOS system, followed by the role that ROS plays. The consequences of OXPHOS dysfunction and the value of specific gene knockout models of *C. elegans* will be presented as a rationale to this study, as introduced in Chapter 1. Thereafter, the focus will be shifted to the use of these models to study potential therapeutic interventions, followed by the aim, objectives, and experimental strategy of this study.

2.2 MITOCHONDRIA AND THE OXPHOS SYSTEM

Mitochondria are intricate, dynamic organelles found in most eukaryotic cells with their most important function being to generate ATP for metabolic energy. Mitochondria contain their own multi-copy genome (mtDNA), with its own genetic code, and replications and expression machinery, located in the mitochondrial matrix. The mammalian mitochondrial genome is transmitted solely through the female germ line. The double-stranded mtDNA is a circular molecule and is 15 – 17 kb (*C. elegans* is 13.8 kb) in size (DiMauro & Andreu, 2000).

As mentioned in Chapter 1, mitochondria supply the cells with the majority of energy needed for day-to-day life and functioning of cells (Siekevitz, 1957). For this, and as illustrated in Figure 1.1, the mitochondrion contains the oxidative phosphorylation (OXPHOS) system. This system uses the reducing equivalents produced from carbohydrate- (NADH) and fatty acid catabolism ($FADH_2$), to charge the inner mitochondrial membrane through four enzyme complexes (complexes I-IV). This forms the electron transport chain (ETC) – to finally convert ADP to ATP via complex V. The mitochondrial matrix is encircled by a double-membrane system, which consists of an inner mitochondrial membrane (Reinecke *et al.*) and an outer mitochondrial membrane (OMM) that are separated by the intermembrane space (Reinecke *et al.*, 2009; Zhao *et al.*, 2005). The inner membrane forms folds (cristae), which extend into the interior of the organelle. These components play important functional roles and the matrix and inner membrane represent the major working compartments of mitochondria. Investigations on mitochondrial dysfunction and related diseases, such as neurodegenerative disease, underline the importance of the mitochondria for healthy aging and disease resistance (Cooper *et al.*, 2007).

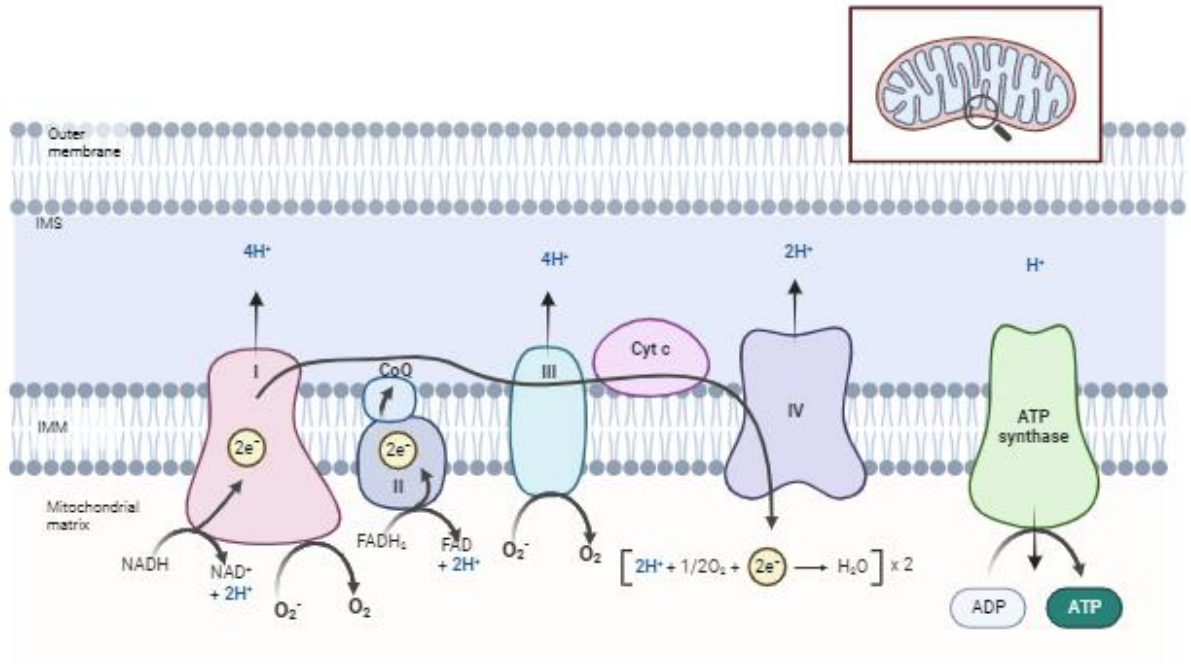

Figure 2.1: An overview of the OXPHOS system. The ETC consists of four enzyme complexes, complex I-IV, which drive the formation of ATP in the OXPHOS system. Complex V finally produces the ATP by ATP synthase activity, and all of these complexes are located in the intermembrane matrix (IMM). In the ETC, electrons enter from NADH at complex I, from succinate at complex II and are then transported to ubiquinone. Complex III transports electrons from reduced ubiquinone to cytochrome c and is carried from cytochrome c to molecular oxygen by complex IV. With this transportation of electrons across the IMM into the inter-membrane space (IMS), it creates a proton gradient that steers the ATP production by complex V. The leaking of electrons to oxygen at CI and CIII are also indicated. Adapted from Zhao et al., 2019 by BioRender.com (2022). Retrieved from https://app.biorender.com/biorender-templates.

2.3 REACTIVE OXYGEN SPECIES

ROS are continuously generated in human cells by various normal essential endogenous systems, or from external exposure to different physicochemical conditions, such as environmental pollution, UV radiation, certain drugs or pesticides, and cigarette smoke (Devasagayam, 2004; Ebadi, 2001). The majority of ROS are generated by normal cellular metabolism in the OXPHOS system. It may cause damage to macromolecules within the cell, which can accumulate over time and lead to dysfunction at organismal and cellular levels (Machiela *et al.*, 2016). Certain changes are considered normal, as that related to aging. However, these changes can also be influenced by genetics and environmental changes which, over time, can manifest as diseases (Lobo *et al*., 2010; Miranda-Vizuete & Veal, 2017).

ROS and reactive nitrogen species (RNS) have a higher reactivity than molecular oxygen (Kwok *et al.*, 2006). ROS include free radicals such as superoxide radical (O_2^-), hydroperoxyl radical (HO_2^-), hydroxyl radical (HO^-) and peroxyl radical (ROO^-), as well as non-radicals, namely, hydrogen peroxide (H_2O_2), singlet oxygen ($^-O_2$), and hypochlorous acid (HOCl) (Murrant, 2001). By definition, free radicals are atoms or molecules that can survive on their own, that carry one or more unpaired electrons (Barry, 1991). Molecules are more stable when they have two electrons paired together in orbitals of opposite direction of spin. This means that free radicals are generally less stable than non-radicals. Free radicals can adversely alter DNA, protein and lipids by disturbing their structures, and have been implicated in aging and a number of human diseases (Cooke *et al.*, 2003).

As mentioned before, the source of endogenous ROS is well established in normal cellular metabolism. These cellular processes account for the background levels of oxidative DNA damage detected in normal tissues. In the ETC there is a possibility of leaking electrons to oxygen at CI and CIII, leading to superoxide generation (Cooke *et al.*, 2003), as illustrated in Figure 1.1. Fortunately, the mammalian organism has provided protection against potentially damaging effects of ROS, namely antioxidants. As seen in Figure 1.2, numerous antioxidants exist, including enzymes such as superoxide dismutase (SOD, which reduces $O_2^{-}\cdot$ to H_2O_2), catalase, and glutathione peroxidase (GSH, which reduces H_2O_2 to H_2O). If the balance between ROS production and antioxidant capacity of the cell is disturbed, this may lead to oxidative stress (Thannickal & Fanburg, 2000). This leads to further mitochondrial dysfunction, which may lead to even more production of ROS (the so-called "vicious cycle") and finally triggers cell death; hence, aging and diseases (Dilberger *et al.*, 2019). It is estimated that ~2% of electrons passing though the ETC leak to oxygen to form superoxides (Turrens, 1997). H_2O_2 is less reactive than other ROS species but it can react with free iron (Fe^{2+}) in the Fenton reactions and in turn produce hydroxyl radicals which is one of the most reactive oxygen species. This means the removal of these species is very important for the protection of cells and to avoid oxidative damage (Radi *et al.*, 1991).

Considering that mitochondria have numerous functions beyond ATP production, ROS is of particular interest for mitochondrial pathogenesis (Hu *et al.*, 2018). In the mitochondrion, ROS are produced as a by-product of ETC reactions. It is important to indicate that healthy cells need ROS, since ROS also play an important role in signalling and responses (Miranda-Vizuete & Veal, 2017). Miquel and Fleming (1980) first described the "oxygen radical-mitochondrial injury hypothesis of aging", which suggests that the mitochondrion is the main target of radical damage (Miquel *et al.*, 1980). If mitochondria have one or more defects of the many nuclear and mitochondrial proteins, they will cause the mitochondria will dysfunction. The relationship between

mitochondrial function, ROS production, ROS damage and the phenomenon of a clinical phenotype of ageing are still poorly understood *in vivo*. Thus, topics on disease and therapies that may be caused by ROS are increasing.

2.4 ANTIOXIDANTS

Cells contain numerous essential antioxidant mechanisms to prevent the damage caused by ROS (Weydert, 2010). As illustrated in Figure 2.2, and relevant to the disease model used in this study, the first line of defence against ROS *in vivo* is SOD. This enzyme is available in the mitochondrion, cytoplasm, and extracellular space, since superoxide detoxification is required at the area of generation (Van Raamsdonk, 2010). Glutathione peroxidase (GPx), catalase (CAT) and peroxiredoxin (PRX) are a combination of enzymatic detoxifying systems that can convert H_2O_2 to H_2O (McCord, 1971). Superoxide radicals are converted to hydrogen peroxide and oxygen through SODs; hydrogen peroxide is converted into water through catalase and peroxidase. The consequence of this is that superoxide and hydrogen peroxide are then converted to water. GPx requires several co-factors and proteins (Weydert, 2010). SOD enzymes are thoroughly compartmentalized, such as manganese-containing superoxide dismutase (MnSOD), copper- and zinc-containing superoxide dismutase (Cu/ZnSOD) and extracellular SOD. As seen in Figure 2.**1**2, which provides an overview of antioxidant and ROS metabolism in the animal model for this study, SOD-2 and SOD-3 are in the mitochondrion, and SOD-1 and SOD-5 are in the cytoplasm. In *C. elegans,* it was shown that SOD activity levels either remain unaltered during their lifespan, or linearly increase with age. This phenomenon, apparently, eliminates the possibility that a significant decrease in SOD activity contributes to oxidative damage in aging organisms (Vanfleteren, 1993).

Thus, there are various forms of these enzymes, in addition to chemical antioxidants, in different compartments of the cell that modulate oxidative stress (Weydert, 2010). Unfortunately, these antioxidants alone cannot prevent the pathophysiology of disorders of mitochondria, requiring additional interventions. There are also other organic antioxidant molecules/peptides to combat ROS, such as glutathione, MTs and vitamins. Glutathione can reduce peroxides and free radicals, and MTs can scavenge for hydroxyl radicals and superoxides. Vitamin C and vitamin E, respectively, have been shown to scavenge oxygen radicals, protect membranes from radical formation and reduce the harmful effects of oxidative stress (Mrityunjaya *et al.*, 2020; Niki, 1987; Vašák, 2005).

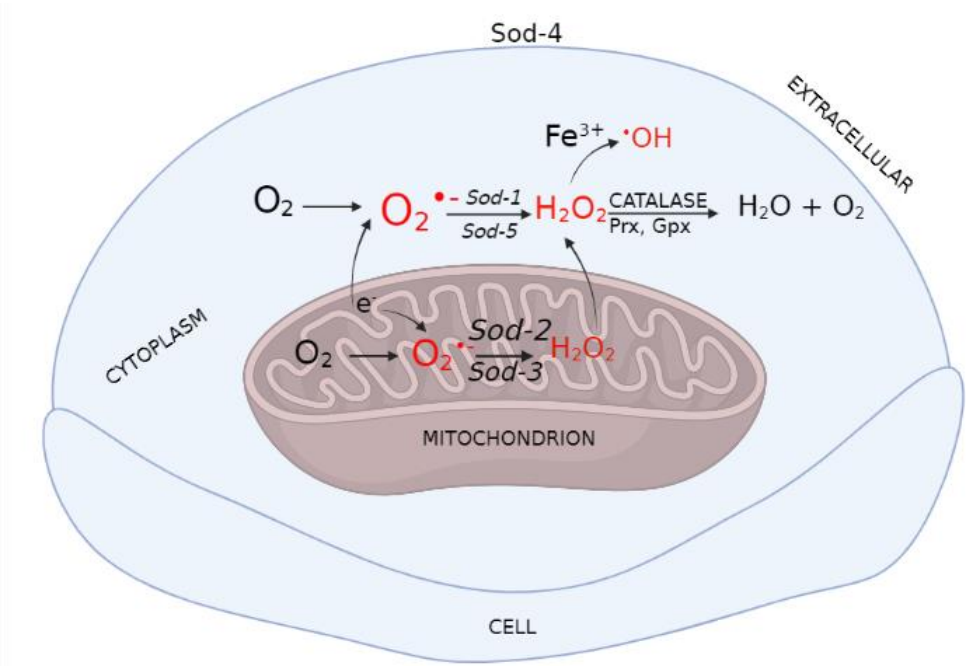

Figure 2.2: Basic pathways of ROS production and antioxidants in *C. elegans*. Primary pathways of ROS production and antioxidants in a *C. elegans* cell. The ROS molecules (in red) are converted to less reactive molecules through antioxidants. There are five different sod enzymes that converts superoxides to H_2O_2 and are found in different cellular compartments. Catalase, peroxidoxin (Prx) and GPx convert H_2O_2 to H_2O and O_2. Immediate detoxification of H_2O_2 is required as it can become oxidised to form a potent free radical •OH. An increase in these free radicals may lead to damage of the DNA, RNA, proteins and lipids, and high ROS can cause oxidative stress (Adapted from Johnston & Ebert, 2012).

2.5 MITOCHONDRIAL DISEASE

Mitochondrial diseases (MDs) are a clinically diverse group of disorders. They can appear as consequences of dysfunction in the OXPHOS system, or caused by mutations of genes that are encoded by either nuclear DNA (nDNA) or mitochondrial DNA (mtDNA). MDs can affect different organs, or they can affect only a single organ. A feature of MDs is that they may occur at any age and with different phenotypes, often resulting in broad phenotypes (Cohen, 2019; Gropman, 2004).Variants in any of the genes of these complexes of ETC that encode for any of the enzymes that are needed, can result in MD. If there is a mutation in the affected enzyme complex, the complex may not work properly and can lead to a decrease in ATP. This can lead to a wide range of symptoms, but most often muscle, development or nervous system are greatly affected (Gorman *et al*., 2015).

Notably, with MD patients who have a mtDNA mutation, it is common that their clinical features fall into a clinical syndrome type, such as mitochondrial encephalomyopathy, with lactic acidosis and stroke-like episodes (MELAS) (Gorman *et al*., 2015). MDs can be classified into two main groups: primary and secondary mitochondrial diseases. Primary MD is diagnosed with mutation in a (mtDNA or nDNA) gene that encodes for OXPHOS structural proteins or genes that directly affect the OXPHOS system, such as import proteins or mtDNA housekeeping genes (Chinnery, 2014; Gorman G.S., 2015). Secondary MDs are also clinically and biochemically diagnosed with the disease, but the genes involved don not encode for structural or regulatory OXPHOS proteins and can be presented with various hereditary non-mitochondrial diseases or dysfunction in the processes. Secondary MD may also occur due to environmental effects that can cause oxidative stress or dysfunction of bioenergetics metabolism.

Thus, a key difference is that primary MD can only be inherited, but secondary MDs can be inherited or acquired (Niyazov *et al.*, 2016). To distinguish between primary and secondary MDs is still very challenging and requires genetic investigations in both mtDNA and nDNA. Important aspects for MDs are effective diagnosis as early as possible because of the severity of the diseases. Unfortunately, to date, there are only a few effective treatments and no known cure for MD, and as expected, these processes are not straight forward (Kornblum *et al*., 2023).

During recent years, thanks to the development and more cost effective (next generation sequencing (NGS) technologies, there has been remarkable improvement in genetic testing. This contributed to new knowledge of the genes involved in mitochondrial diseases in general. The growing number of cases related to mitochondrial dysfunctions and the genotype to phenotype identification will potentially help to understand more of the mitochondrial disorders (Fernandez-Vizarra & Zeviani, 2021). An example of neurodevelopmental disorder found that brain development is delayed as a consequence of inflammation that induces oxidative stress and mitochondrial damage, which then increases oxidative stress and results in further cellular damage (Zawadzka *et al*., 2021).

2.6 CELL BIOLOGICAL CONSEQUENCES OF OXPHOS DYSFUNCTION IN MITOCHONDRIAL DISEASE

OXPHOS dysfunction almost always leads to disease and the most common form of inherited metabolic disorders is mitochondrial disease. The dysfunction in mitochondrial diseases is

complicated and usually involves genetic mutations in mtDNA and/or nDNA, or as indicated before, it can also be caused by external factors such as, exposure to certain chemicals (Gorman *et al.*, 2016). Usually, mitochondrial diseases are a consequence of a defect or dysfunction in the process of cells producing energy (ATP). However, there is a plethora of other cell biological consequences that may be initiated from OXPHOS dysfunction, as reviewed extensively before (Reinecke *et al.*, 2009). These include, in addition to reduced ATP production, a change in mitochondrial membrane potential and the various functions associated with it, such as ion transport, redox state, ROS production, apoptosis, and, from these cellular modulators, retrograde signaling to the nucleus. From this signaling and nuclear response, various anterograde responses (gene expression) can then be initiated that can be protective – such as mitochondrial biogenesis, or antioxidant responses such as MT expression – or differentiation, or cell death. The responses depend on a number of factors, including tissue type, severity of the dysfunction, genetics and cellular health (Reinecke *et al.*, 2009).

These responses are a major reason for the heterogeneity found in mitochondrial diseases and partly explain its clinical heterogeneity, and why the diseases can occur at any age in a variety of clinical symptoms patients. MD can influence any organ or tissue and then include multiple systems. The organs that require high energy and depend on aerobic metabolism are often ultimately affected the most, leading to high morbidity and mortality. Thus, the diversity of these clinical consequences of MD means that the management and treatment thereof is very difficult. Finding the molecular mechanisms that are involved for this wide variety of disease manifestations remains challenging (McFarland *et al.*, 2010).

Whether the variants occur in nDNA or mtDNA of the OXPHOS system, the effects of MD are damaging and dangerous if left untreated. The MDs are mostly characterized by impaired features of energy demanding tissues and are thus generally multi-systemic (DiMauro & Schon, 2003; Haas *et al.*, 2007). Mitochondrial dysfunction is fundamental in many diseases and the involvement has been recognized in mammalian models (Koopman, 2016). Typically, when cells age, certain functions decline, and this may cause reduced ATP and increased ROS. The responses to mitochondrial dysfunction vary between patients and tissues, but the biochemical phenotypes mainly include increased ROS, altered redox status (NADH/NAD+ ratio), decreased energy (ATP), changes in the Ca^{2+} homeostasis and disruption of the mitochondrial membrane potential (Reinecke *et al.*, 2009).

The normal process in the mitochondria of free radical production is partly responsible for damaging cells and DNA, especially mtDNA because it is near the source of production. Because

the mitochondrion is the primary location in which ROS damage happens, there is also a well-known hypothesis that mitochondria play a role in aging. When variants occur in OXPHOS, as in primary MD, it causes protein dysfunction and a decrease of normal ATP levels, and may also have increased free radical production (Cohen, 2019). This then leads to ROS causing damage to mitochondria, ultimately causing further mitochondrial dysfunction in a vicious cycle, and interrupting a great number of cellular functions in energy demanding tissues, leading to the pathologies associated with MD (Dues *et al.*, 2016). Over the years, mitochondrial diseases have been characterized with different nomenclatures and with different phenotypic presentations, such as MELAS. MD rarely have a phenotypic presentation correlation with specific enzymatic, biochemical or genetic findings (DiMauro *et al.*, 2013).

When considering the disease model in this study, *C.elegans*, mutations in OXPHOS mutants have been identified previously, for example, *gas-1* which is an ortholog of the bovine 49-kD protein of CI (Kayser *et al*., 1999). CI is the largest complex and is one of the points of entry through which electrons flow to the respiratory chain and one of the proton pumps. Other mitochondrial mutants that have been identified are variants in CII is *mev-1* and a CIII variant is *isp-1*. They have defects in other parts of the ETC, and *isp-1* mutants show a decreased rate of CI and CII function (Falk *et al*., 2006; Kayser *et al*., 1999). Further, evaluating and identifying OXPHOS mutants in *C. elegans* may help with potential screening of treatments or other strategies that can be considerd at when looking at mitochondrial diseases. What is notably lacking in these models is ROS production data.

2.7 REDOX MODULATION, REACTIVE OXYGEN SPECIES AND MITOCHONDRIAL DISEASE

The key enzyme that is responsible for most of the cellular energy generated by the OXPHOS system is ATP synthase. According to Mattiazzi *et al*. (2004), they found increased ROS production, free radical damage to lipids, and mitochondrial superoxide dismutase activity in the ATP synthase mutant cells linked to a decline in mitochondrial respiration. Noting that these mutant cells showed an increase in ROS, they treated them with antioxidants, which resulted in enhanced mitochondrial respiration and ATP synthesis (Mattiazzi *et al.*, 2004). Variants can occur in any cell and may lead to changes in the structure of proteins that are encoded or complete loss of the protein expression resulting in cell damage (Lodish *et al.*, 2008). The ETC complexes can be inhibited and this may cause a biochemical threshold effect, where this halt will cause a flux of respiration to collapse, which may result in damage to the cell (Obre & Rossignol, 2015). If the

mitochondrial redox homeostasis is decreased, it can lead to inflammation, in particular mitochondrial inflammation that may be caused by an increase in ROS. It has been proposed that mitochondrial dysfunction and an increase in ROS may induce inflammation, which acts as a feedback system within a stressful environment (Patergnani *et al*., 2021).

Furthermore, Patergnani *et al*. (2021) showed a new concept, that mitochondria act as a regulator and checkpoint for the inflammatory process. Mitochondrial ROS may influence and regulate a few aspects regarding mitochondrial inflammation; the mitochondrial importance in reducing or combating mitochondrial ROS, and possibly assisting in reducing the effects of inflammatory-related diseases (Patergnani *et al*., 2021). Mitochondrial dysfunction during the ETC processes can lead to ROS leaking through the IMM, which may activate numerous cell death signalling pathways (Xu, 2019). One result of excess ROS production can lead to the induction of macromolecular damage, which results in further dysfunction and ROS production, and ultimately in cell death (the so-called vicious cycle). Overwhelming evidence suggests that ROS contributes to the pathophysiology of many non-communicable diseases, such as cardiovascular disease (Tan, 2001), neurodegenerative diseases, such as Parkinson's disease (PD), mitochondrial dysfunction and cancer (Xiao *et al*., 2022).

2.8 THERAPEUTIC INTERVENTIONS FOR MD THAT TARGET REDOX MODULATION AND ROS

Treatment and management of patients with MDs is still challenging. Treatment or improvement of mitochondrial disease is still very complex due to the variability of mitochondrial dysfunction phenotypes. Currently, treatment for mitochondrial diseases is mainly to improve mitochondrial function and improve the quality of life of the patients, and usually treatment involves cooperation of different types of interventions. Some dietary restriction is used for some of the diseases, but the dietary restriction alone is not effective and the extent to which dietary restrictions impact the mitochondrial function remains unclear (Colman *et al.*, 2014; Miwa *et al.*, 2022). Another approach that is evident from the pathophysiology of MD is the use of antioxidants and exercise. For the most common paediatric form of MD, called Leigh syndrome, these and other therapeutic interventions have been reviewed by Tiet *et al*. (2021), with the targeting of redox modulation still being the most promising approach. Several examples and approaches for therapeutic interventions targeting redox modulation in literature exist, and relevant to the rationale for this study and provided in Chapter 1, is that it was hypothesised that MT expression can be responsive to a deficiency of CI and that MT may be involved in combating ROS (Zeitoun-Ghandour *et al*., 2011). It was initially reported using a rotenone-generated model for CI deficiency, that MT was

induced and that its expression has a protective outcome to the toxic effects of rotenone (Reinecke, 2006).

The role of MTs to protect against the damaging effects of ROS has been investigated in mitochondrial diseases and are still considered as a potential therapeutic option for mitochondrial disease where ROS are proven to be contributing to the pathophysiology (Hench *et al.*, 2011; Lindeque *et al*., 2010; Miller *et al*., 2021).

Within cells, a variety of chemical reactions are continuously occurring and the reaction of reduction-oxidation reactions play an important role in maintaining cellular functions, such as metabolic cycles (for example, NAD^+ and NADH conversions), and detoxifying of harmful material (Sharma *et al.*, 2018). There are two highly conserved enzymatic systems that are responsible for maintaining the redox homeostasis and to reduce most forms of oxidative modification proteins; firstly, thioredoxins can be reduced by thioredoxin reductase, which uses NADPH as an electron donor, and glutaredoxins, which consist of small redox enzymes, and they can directly collaborate with oxidized protein thiols and also use NADPH as an electron donor (Holmgren *et al.*, 2005). Both thioredoxin and glutaredoxin systems use NADPH as their electron source, and thus, the cellular redox status for $NADPH/NADP^+$ (Schafer & Buettner, 2001).

The redox status is the balance between oxidized and reduced compounds within a cell, and cells aim to maintain a good electrical balance between a variety of molecules. This is why oxidative stress can occur when the balance of the redox status is disrupted by an increase or a shortfall of either oxidants or reductants, and a strong modulation of its redox status is a critical cellular function (Halliwell & Gutteridge, 2015). In future research, exploring novel therapeutic interventions is warranted, with a focus on leveraging the unique advantages of the *C. elegans* model system, which were not addressed in the present study.

2.9 *C. ELEGANS* AS A MODEL ORGANISM

Other than the vertebrate model organisms, such as mice, there are established invertebrate models for research, including *C. elegans*. In 1963, Sydney Brenner discovered a small, free-living nematode found worldwide, called *C. elegans*. Adult *C. elegans* are usually about 1-millimetre long as can be observed through microscopes (Fig 2.3). In the laboratory, *C. elegans* are grown on agar plates containing *Escherichia coli* (*E. coli*) OP50. Other properties of *C. elegans* include transparency, self-fertilizing hermaphrodite, short lifespan (2-3 weeks depending on the temperature) and easy to maintain in the laboratory (Brenner, 1974). *C. elegans* grow from egg to egg-laying, to reproductive adult within 4-5 days and increase in size throughout their lifespan, with four larval stages, namely L1 - L4. *C. elegans* was the first multicellular eukaryotic

organism to have its genome sequenced and can be genetically modified and maintained through self-propagation progeny without mating. Furthermore, the mitochondrial genome of *C. elegans* – in its structure more than its size (13794 bp) – is comparable to the human mitochondrial genome (16649 bp) (Corsi *et al.*, 2015; Leung *et al.*, 2008).

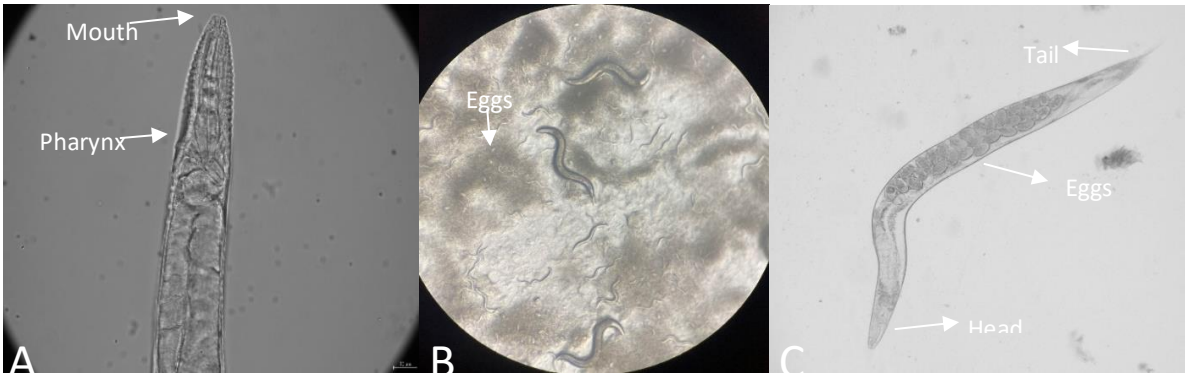

Figure 2.3: Images of *C. elegans*. (A) A magnified view of *C. elegans*, at the top is the mouth and the pharynx. The pharynx is a neuro-muscular pump and is used to ingest food, grind it up and transport further into the intestine. (B) *C. elegans* feeding on a lawn of bacteria in a petri dish. Eggs and nematodes of different ages. (C) Adult *C. elegans* with plenty of eggs inside. The head is at the bottom and the tail is at the top (WormBase, 2022). Photos (A) and (C) were captured with a Zeiss LSM 980 microscope and (B) was taken with cell phone and Nikon stereo microscope.

Uunder unfavourable conditions such as starvation, *C. elegans* goes into a compensatory development stage called *dauer* larvae. During this stage, *C. elegans* can survive up to several months without food and the development is halted until maturation when replenished nutrients are provided. *C. elegans* can be either a self-fertilizing hermaphrodite, or male. The majority of laboratory *C. elegans* populations are hermaphrodites (Corsi *et al.*, 2015). Specific properties of *C. elegans* should be noted when considering it as a disease model. *C. elegans* have an invariant cell number and development, and the ability to reduce gene activity by feeding RNA interference (RNAi) (Corsi *et al.*, 2015). Most models/strains are still incompletely characterised and have some flaws when comparing to human disease models; working with *C. elegans* thus also has some disadvantages. The small size of the animal has challenges; thus, experimental manipulation in individual tissues is difficult. *C. elegans* also lacks specific tissues, such as brain and blood.

2.10 *C. ELEGANS* AS A MODEL TO STUDY ROS

It was already motivated that the mitochondrion and its functions are essential in life, and studying the diseases associated with it, as well as ROS, are challenging. To address these challenges other animal model systems, such as mice and yeast models were established to study diseases associated with mitochondrial dysfunction and ROS (Ruzzenente, 2016). Grad and Lemire (2004) have modelled a knockout of a subunit of CI (NDUFV1) in *C. elegans*, which displayed comparable biochemical features to human cells. These *C. elegans* mutants allow for exploring underlying mechanisms of a CI defect, including ROS (Grad & Lemire, 2004). Ventura *et al*. (2006) further reported that some long-lived mitochondrial *C. elegans* mutants are a powerful model to study human mitochondrial diseases, to explore the involved pathways and to test compounds or antioxidants for treatment of diseases. Two good mitochondrial mutants that were shown to have a shortened lifespan and dysfunctional mitochondria in *C. elegans* are *mev*-1(*kn*1), which contain a missense allele in the gene that codes for a cytochrome b subunit of succinate dehydrogenase (CII), and *gas*-1(*fc*21), with a mutation in the 49-kDa subunit of CI (Senoo-Matsuda *et al.*, 2003).

As already described, ETC subunits are key in the production of ROS. A malfunctioning of any of these subunits (notably CI and CIII) may lead to increased ROS. According to Senoo-Matsuda (2001), *mev-1* phenotypes result in an overproduction of ROS. *Mev-1* phenotypes include a short lifespan and increased SOD levels. There are several of the mutant *C. elegans* strains with variants in different OXPHOS subunits. For this study, we will be focussing exclusively on a variety of *C. elegans* models that have OXPHOS variants and thus potential increased ROS production.

Increased ROS caused by mitochondrial dysfunction may further lead to neurodegeneration, cell death and damage to nuclear DNA and mtDNA. ROS damage and the full complement of its consequences are poorly understood. This is why it is important to elucidate the mechanisms of ROS and the role of protective mechanisms *in vivo,* such as in *C. elegans* (Bansal, 2012; Senoo-Matsuda *et al.*, 2001). In addition to the CI and CII mutants described before, MQ130 worms that have a mutation in *clk-1*, which encodes a hydroxylase involved in the synthesis of ubiquinone (coenzyme Q), showed a decrease in OXPHOS function and an increase in ROS production (Schaar, 2015).

A typical approach is to study animal behaviour that corresponds to the behavioural differences with biological mechanisms. Behaviour represents how organisms interact with and/or adapt to their environment. The nematode has become one of the most widely used model organisms for various aspects of biology. Some of these *C. elegans* mutant strains, in addition to others, will be

investigated to evaluate the relative potential of these mutants to study the effects of ROS and future therapeutic interventions. An interesting observation in these models, and a potential complication, is that an increase in lifespan in *C. elegans* with impaired OXPHOS systems is observed (Falk *et al.*, 2008; Van Raamsdonk *et al.*, 2010). It was later shown that this could be due to the effect of FUdR (5'-fluorodeoxyuridine) (Anderson *et al.*, 2016). FUdR is used to sterilize *C. elegans* to do lifespan analysis and it was advised to not use FUdR in studies that include stressed *C. elegans*, aging studies, or when different genotypes are compared.

In addition, a common method for measurement of intracellular ROS utilizes the fluorescent properties of lipophilic molecules, such as dihydrodichlorofluorescein diacetate (H_2DCFDA). The membrane-permeable dyes enter the living cells, the intracellular esterases cleave to the acetate moiety and holds the H_2DCF inside the cell. ROS then oxidizes the non-fluorescent H_2DCF to yield the fluorescent dichlorofluorescein (Bass *et al.*, 1983; Keston & Brandt, 1965). Another fluorescent dye measurement of ROS is MitoSOX, this is a dehydroethidium (DHE) molecule that targets superoxides in the mitochondria. The O_2^- oxidises the DHE and ethidium is formed, which is a fluorescent compound and can be visualized with a confocal microscope or Fluorescence-Activated Cell Sorting (FACS) analysis (Dingley *et al.*, 2010; Zhao *et al.*, 2005).

2.11 PROBLEM STATEMENT, AIMS AND OBJECTIVES

Taking into account that mitochondria have numerous functions beyond ATP production, ROS is primarily generated in the mitochondria. Miquel and Fleming (1980) first described the "oxygen radical-mitochondrial injury hypothesis of aging", which suggests that the mitochondrion is one of the main targets of radical damage. The relationship and understanding of mitochondrial function, ROS production, ROS damage and how it is expressed in the clinical phenotype is still very limited.

Phenotypic characteristics and behaviour require frequently measuring numerous parameters that quantify movements, posture and development (Yemini *et al.*, 2013). In *C. elegans,* the arrested phenotypes of knockout animals showed consequences and are observed in the mitochondrial mutants, such as short life span and sterility (Ventura *et al.*, 2006). For example, the complex I variant may result in reduced brood sizes, decreased respiration, decreased energy and slow growth. Grad and Lemire (2004) suggested that complex I dysfunction causes disease, and it may be because of the increased production of ROS, and thereby interfere with the function of the OXPHOS system through DNA damage, lipid peroxidation etc. Thus, investigating certain *C. elegans* mutants and their ROS production is very important to understand and to evaluate it as a model for further research and potential therapeutics.

Evaluating ROS production in OXPHOS KO strains of *C. elegans* can provide valuable insights into the role of ROS in cellular physiology and disease and may lead to the development of therapeutic strategies for targeting ROS-mediated processes. Limitations in previous studies at the North-West University (NWU), where CI disease models in mice were studied were; (i) ROS analyses were not tissue-specific, (ii) tissue samples also made it very hard to get a direct measurement of ROS, which also could not be confirmed, (iii) because of the inherent behaviour of mice, high variability was observed in the phenotypes (Miller, 2020). Thus, these limitations guided this study to investigate the appropriateness of *C. elegans* to investigate the effect of redox modulators such as MT for scavenging of ROS.

To address the mentioned limitations, this study aimed at using available models of OXPHOS dysfunction of *C. elegans* to analyse mitochondrial dysfunction and ROS. The high homology between humans and *C. elegans* genes makes it possible to relate to human diseases (Maglioni & Ventura, 2016). The models that will be evaluated are all strains that could be obtained with a documented genetic variant in the OXPHOS system. The study proposed to evaluate these strains for ROS production, with the objective of identifying those with increased ROS-production as future *in vivo* models for redox modulation/antioxidant interventions.

2.12 AIMS, OBJECTIVES AND EXPERIMENTAL STRATEGY

The *aim* of this study was the evaluation of ROS production in a selected number of OXPHOS KO strains of *C. elegans*. Five *objectives* were identified to reach this aim as listed below, with the experimental strategy to achieve these objectives summarised in Figure 2.4:

1. Identify from literature the available OXPHOS-deficient *C. elegans* strains and controls.

2. Acquisition of selected strains and establishing general procedures for the culturing and maintaining of *C. elegans*.

3. Confirm the genetic knockout in the selected strains using molecular genotyping analysis.

4. Biochemical characterization of selected strains using respiration, behavioural and other phenotypical characteristics.

5. ROS measurement of mitochondrial ROS in the selected strains.

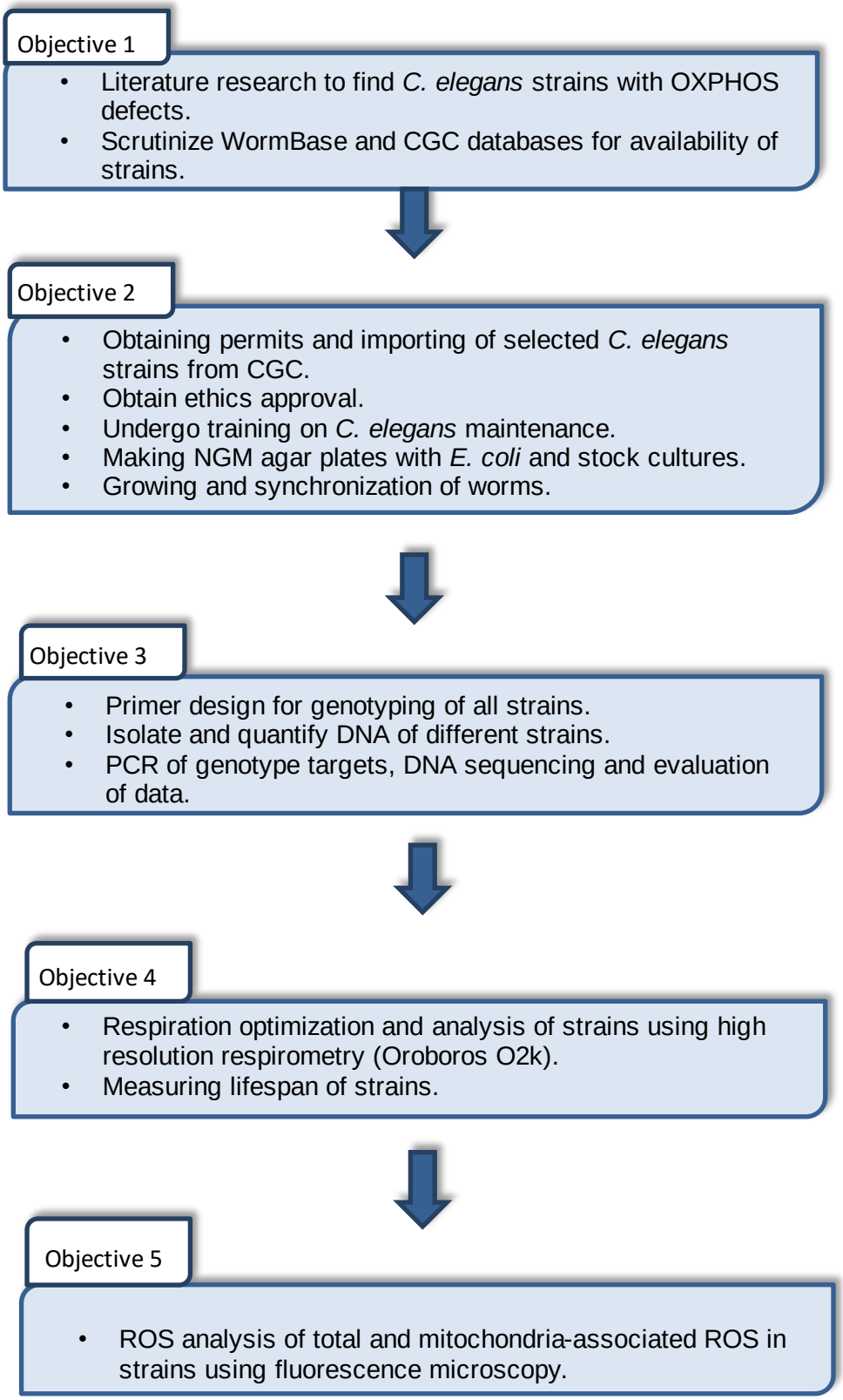

Figure 2.4: The experimental strategy summary that is utilized in this study.

CHAPTER 3 MATERIALS AND METHODS

For *C. elegans* OXPHOS-deficient strain selection, an extensive literature review was done to identify the available strains as well as controls. The key search terms using Scopus (www.scopus.com/home.uri) and PubMed (https://pubmed.ncbi.nlm.nih.gov/), were search combinations of "*C.elegans*/nematode", "respiratory chain deficiency/knockout", "OXPHOS deficiency/knockout", and "ROS". OXPHOS deficient models were compared and established strains that had a clear deficiency in a variety of subunits with a potential of generating ROS were considered. The literature review was also duplicated using WormBase. WormBase is an online international consortium of different scientists providing the research community with varied information on *C.elegans*; from genetics to the biology of *C. elegans* (WormBase, 2022). In addition, wild-type (N2) control, which has the same genetic background as the knockout strain, was also selected, as well as a potential positive control for ROS generation (SOD knockout). Table. 3.1 contains the list of selected strains, genes and complexes involved.

In the context of *C. elegans* for example, the notation "mev-1(kn1)" refers to a specific genetic mutation in the mev-1 gene in a *C. elegans* strain. Example of the components:

- *mev-1*: This is the gene symbol. Genes in *C. elegans* are often assigned specific symbols to represent their names.
- (kn1): This is an allele designation, indicating a specific mutation in the *mev-1* gene. The (*kn1*) suggests that it is a particular allele or variant of the *mev-1* gene, and "*kn1*" is likely the identifier given to this specific mutation.
- The specific nature and effects of the "*kn1*" mutation would need to be referred to in the genetic databases, as different mutations can have various impacts on gene function and organismal phenotype.

Table 3.1: List of selected *C. elegans* strains with information provided by the Caenorhabditis Genetic Centre (CGC), Minneapolis, USA.

Gene	Strain	Name & enzyme complex involved
Wild-type	N2	Caenorhabditis elegans wild isolate.
isp-1(qm150)	MQ887	An iron-sulfur protein and is involved in mitochondrial electron transport from ubiquinol to cytochrome c (CIII).
nuo-6(qm200)	MQ1333	NADH Ubiquinone Oxidoreductase (CI).
sod-2(gk257)	GA184	Iron/manganese superoxide dismutase and is involved in removal of superoxide radicals (CI, CIII).
gas-1(fc21)	CW152	General Anesthetic Sensitivity abnormal, is involved mitochondrial electron transport (CI).
mev-1(kn1)	TK22	Abnormal Methyl Viologen sensitivity (CII), involved in mitochondrial electron transport.
nuo-1(ua1)	LB25	NADH Ubiquinone Oxidoreductase (CI), involved in mitochondrial electron transport.

3.1 ACQUISITIONS OF STRAINS AND MAINTENANCE

For the import of nematodes, an import permit (No:13/11/30/2/0-202007003664) had to be acquired for selected strains through the Department of Agriculture, Forestry and Fisheries (DAFF) as required by Section 20 of the Animal Disease Act, 1984 (Act no35 of 1984). The necessary ethical approval for this study was obtained from the AnimCare Ethics Committee of the NWU in 2021 with approval number NWU-0041521-A5. The imported strains are listed in Table 3.1. Upon arrival of the nematodes, general procedures for culturing and maintaining of these worms were established with training received from a nematode scientist, Dr Gerhard du Preez, Division of Zoology, NWU.

All the strains used in this study were obtained from the Caenorhabditis Genetic Centre (CGC), Minneapolis, USA. Nematode growth media (NGM) agar plates, seeded with *Escherichia coli* OP50 (*E. coli* OP50) as food source, were used for nematode maintenance at 20˚C. The *E. coli* OP50 is a uracil-requiring mutant type of *E. coli* and is used to prevent overgrowth of the bacteria in the plates for the visualizing of the nematodes. To ensure that the different strain plates did not mix, the plates were marked at the bottom with the strain name and date. They were also kept

separately in dividers in the incubator. After every 2-3 weeks, new *E. coli* plates were made and every strain was transferred to the new *E. coli* plates, either by picking the worms up separately or chunking a piece of agar and placing it on the new *E. coli* plate. Plates were then wrapped with para-film and stored or used. All of the plates were kept for at least 3-6 months as neglected worms/plates can survive for several months if they are not dried or contaminated (Corsi, 2006; Fay, 2013; Stiernagle, 1999).

3.2 PREPARATION OF NGM AND SEEDING PLATES

C. elegans were maintained in the laboratory on NGM agar plates. Different sizes were used according to the objectives. For Luria broth (LB), dissolve 0.5g casein peptone (Biolab, Code #CAP10500), 0.25g yeast extract and 0.5g NaCl (NaCl; Melford laboratories, CAT #S0520) in 50 ml dH2O and autoclaved for 20 min at 121 °C. For M9, 6 g of Na2HPO4; 3 g of KH2PO4 (KH2PO4; Labchem, CAT #7778-77-0); 5 g of NaCl and 0,25 g of MgSO4·7H2O (MgSO4.7H20 (Labchem, CAT #10034-99-8); were dissolved in 1 000 ml of water, in a 1 000 ml flask. For NGM 2,5 g of casein peptone; 17 g of bacteriological agar; 3 g of NaCl; were dissolved in 900 ml water in a 1 000 ml flask and autoclaved for 20 min at 121 °C. After cooling down to 55 °C, the following were added in sterile solutions: 1 ml of cholesterol stock solution (0.5 g/l); 1 mol/l calcium chloride stock solution; 1 mol/l magnesium sulphate stock solution; 1 mol/l potassium phosphate buffer; and filled up to 1 000 ml with sterile water. Portions of NGM agar (about 20 ml to 25 ml) were transferred to sterile Petri dishes (Brenner, 1974 & Corsi, 2006).

Using sterile techniques, approximately 150-250 µl of *E. coli* OP50 liquid culture, were grown to stationary phase, was added to NGM plates. A sterilized steel rod was used to spread the *E. coli*. This equal distribution over the plate resulted in a "lawn of *E. coli*", which aided in visualizing the worms. The *E. coli* OP50 lawn was allowed to grow overnight (inverted) at room temperature (20 °C) or at 37°C for 17 hours; seeded plates stored in an air-tight container can be used for 2-3 weeks (Brenner, 1988). Plates were equilibrated to room temperature when nematodes were added. The strains were subcultured by transferring a chunk of agar (±1 cm2) containing ~10 nematodes to a bacterial lawn of the new plates every 10 days and this process was followed throughout the entire period of this study.

3.2.1 FREEZING AND SYNCHRONIZATION OF STRAINS

Strains were frozen and synchronized according to standard methods (Brenner, 1974). Briefly, freshly starved young larvae (L1-L2 stage) survive freezing best. Worms were frozen in 1.8 ml cryotubes containing sterile S Buffer (0.05 M K_2HPO_4, 0.05 M KH2PO4, NaCl, and 30% glycerine (v/v) (Sigma-Aldrich®, Code: 101094984)). For collection of nematodes, one large plate, which

contained freshly starved L1-L2 animals was washed with 0.6 ml S Buffer for each vial that was frozen (Corsi *et al.*, 2015).

Ensuring the nematodes of the same age were used at the start of all experiments, synchronization was done with bleaching. Worms were washed off the plate with ± 5 ml of M9 media into a conical tube. Using a glass pipette, worms were transferred to a 15 mL conical tube and centrifuged (1000 x g for 30s.) to pellet the worms. About 15 mL of a 20% (v/v) alkaline hypochlorite solution was added to the tube, and mixed gently until a decrease in the number of intact adult worms could be observed. Most of the M9 was discarded without disturbing the pellet. About 7 mL of fresh M9 were added and the eggs were left to hatch overnight at 20 °C while gentle rocking. If there is no food, the larvae will be halted at the L1 stage and can survive for up to two weeks.

3.3 GENOTYPING OF STRAINS

To confirm the published genotypes of the various strains, DNA was isolated from each strain, the area around the mutation was amplified using polymerase chain reaction (PCR), and the amplified DNA fragments were sequenced to confirm the presence of the various mutations. The data, as reported further, was compared to the characteristics and sequence information as reported for these strains (WormBase, 2022-34-5). From the sequenced data, we expected to observe specific genetic variations from the wild-type, such as an insertion or substitution, specific for each strain.

3.3.1. PREPARATION OF NEMATODE LYSATES AND PCR.

For the preparation of a crude lysate as template sample for PCR, the following procedure, based on the procedure supplied by Thermo Scientific Phire Tissue Direct PCR Master Mix (Thermo Fisher Scientific™), was followed for each of the selected strains. The exact content of the kit reagents is given where known. A lysis buffer was prepared using the supplied lysis buffer with the addition and mixing of 1 µL of 10.0 mg/mL proteinase K to 99 µL of lysis buffer. For each strain, one to five worms were picked up and placed in a 3 µL drop of lysis buffer, which was placed in a 0.2 mL PCR tube, followed by mixing. The closed tube was briefly (10s) centrifuged to collect the sample volume at the bottom, and if not used immediately, stored at −80 °C. The tubes were placed in a thermocycler with the following incubation sequence: 65 °C for 1 hr, 95 °C for 30 min., 4.0 °C hold. The heat-deactivation of proteinase K at 95 °C is crucial as it can cleave polymerase enzyme during PCR. This lysate was used directly for PCR, or stored at −80 °C until use.

For the PCR reactions, primers, as listed in Table 3.2, that covered the areas where the genetic variants were located, were designed using SnapGene software (Insightful Science) and synthesised by Inqaba Biotec, Pretoria. Table 3.3. describes the PCR contents in a final volume of 25 µL, and Table 3.4. describes the cycling steps that were used. After the PCR, the products were visualized using ethidium bromide (EtBr) containing agarose gel electrophoresis. For agarose gel electrophoresis, the following reagents were used: agarose E (Conda Micro & Molecular Biology, CAT #8100.01), ethidium bromide, 1 X TBE Buffer (Bio-Rad, CAT #161-0770), Milli-Q® H2O. Since the Phire™ Tissue Direct PCR Master Mix contained a pre-mixed gel loading dye, no additional loading dye was required. Furthermore, 5 µL of the GeneRuler™ 100 bp DNA Ladder (#SM0241, Thermo Fisher Scientific™) was included and the gel placed over a current of 4 V/cm of gel. After completion, the gel was imaged under UV light using the ChemiDoc™ MP system (#17001402, Bio-Rad) and the Image Lab software (v5.2.1).

Table 3.2: The strains and their PCR primer pairs used for genotyping. The forward (Fwd) and reverse (Rev) oligonucleotide primers are indicated in a 5'-3' direction.

Genotype	Primer pair
gas-1 (fc21)	Fwd: ATCGTCTCGATTACGTCTCCA Rev: CTTGTGCCGTATTGAGGAGAT
mev-1(kn1)	Fwd: TTCCAACTGCGATTCTGTGC *Rev: TGCCGTTCGATTTCACCGC*
isp-1(qm150)	Fwd: CAGTCCGCCCGTTGAG Rev: GAGGTTCTCTAGATGAGGCGGAGC
nuo-6(qm200)	Fwd: GGACATGAATACAATCTGAGCG Rev: ACCGTATTCCTGTACGTCGG
sod-2(gk257)	Fwd: AAGCACTCGCTGCCAGAT Rev: ATGAAAAGTTTTCACCG
nuo-1(ua1)	Fwd: ACACGAATCTTGCGGACAGT Rev: CAGGGACTCATTCGCCA

Table 3.3: Contents of basic PCR reaction for genotyping

Component	25 µL rxn
H_2O add to 25 µL	x µL
2X Phire Tissue Direct PCR Master Mix	12.5 µL
Primer Fwd (0.5 µM)	0.5 µM
Primer Rev (0.5 µM)	0.5 µM
Lysate Samples	2 µL

Table 3.4: Cycling steps used for PCR

Cycle steps	Temperature (°C)	Time (min)
Initial denaturation	95	10
Denaturation **Annealing** **Extension**	95 53-63 72	1 1 (34x cycles) 2
Final Extension	72 4	5 Infinite Hold

3.3.2. DNA SEQUENCING AND ANALYSIS

Following confirmation of the correct size of PCR amplification for each strain using agarose gel electrophoresis, the PCR samples were sent to the Central Analytical Facility (CAF) at Stellenbosch University, where the DNA fragments were extracted and sequenced using Sanger (dideoxy) sequencing. The resulting sequencing data (Electropherogram base calling) were provided by this service provider. The raw sequencing data for each genotype was processed by removing any low-quality reads to improve the accuracy of the final sequence and compared to the wild-type reference sequence. Lastly, after the genetic variation was identified, it was compared to databases of known mutations on WormBase.

3.4 HIGH-RESOLUTION RESPIROMETRY

A key potential consequence of a deficiency of any one of the OXPHOS complexes, as reported for the selected strains, is the expected compromise of the functioning of the respiratory chain. Direct measurement of oxygen consumption rate (OCR) as a function of mitochondrial respiration in *C. elegans* are usually performed using worms that are suspended in liquid. In this study, the rate of O_2 consumption was essentially measured in *C. elegans* as described by Hench *et al*. (2011) with some modifications. During high-resolution respirometry (HRR), the changes in oxygen concentration are measured using Clark type electrodes. The Oroboros O2k employs Clark-type oxygen sensors, which consist of a cathode and an anode separated by a gas-permeable membrane. The cathode consumes oxygen in a reaction catalyzed by a platinum surface, and the resulting current is proportional to the rate of oxygen consumption.

The Oroboros O2k enables to assess mitochondrial function by monitoring oxygen consumption rates in real-time. This method provides high resolution and sensitivity, allowing for detailed investigations into the various aspects of cellular respiration. The instrument measures the oxygen concentration in a closed chamber. This chamber is equipped with two or more polarographic oxygen sensors, allowing simultaneous measurements of oxygen concentration at different locations within the chamber. As the biological samples respire, they consume oxygen, leading to a decrease in oxygen concentration. The sensors detect these changes, and the resulting signals are recorded and analyzed (Doerrier *et al*., 2018). Previous studies found that TK22 and CW152 had significant lower OCR compared to N2 (wild-type) (Hench *et al.*, 2011). In this study, we used the Oroboros Oxygraph 2K (Oroboros Instruments GmbH, Innsbruck, Austria), with the software DatLab 7.4.0.4 as described in Taferner *et al*. (2015), with some adjustments.

3.5 METHODS

Before respiration analyses, strains were synchronized and the Oroboros was calibrated using M9 buffer. Oxygen consumption of 3–4-day old adults were measured for each strain (n = 4). Approximately 200 adults, as determined in advance by optimizing the number of worms used in these analyses, were manually picked up and placed into 2.5 ml M9 buffer and washed. The worms were then delivered into the chamber and were kept at 20 °C for ±25 min. The data obtained were analyzed with DatLab 7.4.0.4 (Oroboros Instruments GmbH, Innsbruck, Austria). The slope of the straight portion of the plot was used to derive the oxygen consumption (respiration) rate and normalized to number of worms.

3.6 LOCOMOTION

Locomotion is essential in most living organisms. *C. elegans* behavior is expressed through movement, and understanding the basics of locomotion is critical and gives a foundation of their behavior (Yuan and Horvitz, 1990). A popular approach is to analyze behavior and movement of animals in hope of understanding the interactions in different mutants during movement and if underlying dysfunction or disease influences movement. *C. elegans* moves in an oscillating manner, creating a forward motion by producing S-shaped bends along its body in the dorsoventrall (front to back) direction (Haspel & O'Donovan, 2011; Seddon, 2016).

The understanding of *C. elegans'* locomotion is to understand their crawling behavior, which is the moving of their heads when moving on the surface of the agar gels. This provides a phenotypical comparison between wild-type (N2) and the selected mutant strains, and can answer the question of whether the mutant strains are phenotypically affected by the various dysfunctions. It has been shown that the rate of body movements is a good predictor of lifespan and overall health in *C. elegans* (Gray & Lissmann; Taferner *et al.*, 2015). For these analyses, worms were grown at 20 °C on *E. coli* OP50 under standard conditions. Phenotypical assays were performed using 3–4-day old worms as most phenotypes are more pronounced at this stage. The locomotion was done manually with a microscope. Each worm was placed on a clean NGM plate without food, and given 1 min to settle; after this, the locomotion was recorded for 1 min. Locomotion was measured to quantify the motion of *C. elegans* and measuring the physiological activity in its muscles and neurons. To evaluate the impact of the different variants that occur in the worms. For each strain, 10 worms were used; this was repeated three times, and body bends/min were measured.

3.7 ROS MEASUREMENT

Confocal fluorescence microscopy was selected as method to evaluate ROS, as it provides both qualitative (visual, localization) and quantitative information. Other options, such as fluorescent flow cytometry and microplate assays, were considered, but considering the visual inspection of the localization of ROS in the anatomy of *C. elegans*, it was evident that confocal microscopy had major advantages. Mitochondrial ROS was measured using MitoSOX Red (Invitrogen™, Molecular Probes, CAT# M36008 and M7514). Adult *C. elegans* were transferred to M9 buffer containing 5 µM MitoSOX for about 4 h. After probe incubation, the samples were washed with M9 and allowed ± 30 min to recover. The *C. elegans* samples were then transferred to microscope slides and paralyzed with 1 mM sodium azide (NaN_3, CAT# S2002). For each strain, at least six adult worms were analyzed.

After evaluation of the anatomy and ROS signals that could consistently and comparably be measured, the terminal pharyngeal bulbs were used to quantify the mean fluorescence intensity of this area in *C. elegans.* For each strain, the pharyngeal bulb is analyzed for mainly two reasons: they are easily visualized and have better dye uptake, and they are mitochondria rich but contain less lipid droplets, which are auto-fluorescent and interfere with accurate measurements of mitochondrial fluorescence. As positive control for respiratory chain dysfunction and ROS production, each nematode strain was also incubated with the complex I inhibitor rotenone (5 µM for at least 4 h) (Dingley *et al.*, 2010; Hicks *et al.*, 2012; Zhang *et al.*, 2021). As described by Hicks *et al*. (2012), the final pharyngeal bulb intensity values were calculated as the difference between the intensity values for the wild-type and the knockouts. The intensity of the MitoSOX fluorescence accumulated in the pharyngeal bulb was quantified using ImageJ (Schindelin *et al.*, 2012).

The image analysis setup was equipped with a 40X oil-immersion lens. Fluorescent images were captured using a Zeiss LSM 980 confocal microscope with the same exposure settings. Fluorescence was measured with a 400 nm emission filter, exciting the probes with 405 and 488 nm excitation laser. All live nematodes were analyzed at 4 days of age (Adults). In addition, MitoTracker Green (Invitrogen™, Molecular Probes), incubated at 1 mM for 24 h, was also used in conjunction with MitoSOX to confirm the localization of mitochondrial ROS.

All image analyses was performed using ImageJ (NIH, version 1.53t 24 Aug 2022). Quantification of ROS levels was achieved by manually enclosing the terminal pharyngeal bulb of each image to find the average intensity of the area as described in Dingley *et al*. (2010). Briefly, the visibility of MitoTracker was also measured. ROS were then quantified using the fluorescence emission intensity of each worm (n = 6 per genotype). Animals that displayed bursting, internal hatching and death were excluded from the experiments.

3.8 STATISTICAL ANALYSIS

In the comprehensive evaluation of experiments, rigorous statistical analysis was meticulously carried out employing two powerful tools: GraphPad Prism and Microsoft Excel. The student's t-test, was used for its reliability in comparing the means of distinct sample groups. The significance level of $P < 0.05$ was chosen, ensuring a careful scrutiny of the findings. Additionally, to provide a comprehensive understanding of the data distribution, the calculated results were coupled with the standard deviations (SD), offering crucial insights into the variability around the mean values, thereby enriching the interpretability and depth of the reported outcomes. A One-way ANOVA test allowed for the comparison of three or more groups.

CHAPTER 4 RESULTS

4.1 INTRODUCTION

In this chapter, the results will be described according to objectives as generated using the methods described in Chapter 3. The results are presented in a way that compares the variations as a result of the various genotypes of the nematodes.

4.2 CHARACTERISING THE GENOTYPES OF *C. ELEGANS* STRAINS

Objective 3.1 of this study was to confirm that each of the selected strains encoded the correct genetic variant. In order to achieve this objective, DNA sequencing was performed: 1) DNA was isolated from each strain and the region of each variant was amplified by 2) a PCR reaction. For these reactions, selected conditions were optimised to avoid non-specific amplification or no amplification (the conditions are listed in table 3.1). The PCR products were Sanger sequenced to confirm the reported variant for each of the strains. The characteristics and sequence information were found on WormBase (WormBase, 2022-34-5 Ver.4.2.1).

4.2.1 GENOTYPE ANALYSES

The results of each *C. elegans* strain are displayed in Figures 4.2.1 – 4.2.19. From the sequenced data, specific changes in the form of insertions or substitutions in the relevant genes according to data published in WormBase were scrutinised, in comparison to the wild-type sequence. The electropherograms represented below indicate the fluorescence detection and signal intensity of four colours, each representing a DNA base, and are plotted on the y-axis relative to the time on the x-axis.

The electropherogram is a graphical representation of the fluorescent signals over time, corresponding to the different nucleotides in the DNA sequence. The x-axis represents the migration time of the fragments, and the y-axis represents the intensity of the fluorescent signal. Peaks in the electropherogram represent the termination points of DNA fragments, indicating the position of specific nucleotides in the sequence. The final step involved "base calling," where software analyzed the electropherogram to determine the sequence by assigning each peak to a specific nucleotide. The sequence is then assembled based on the positions of these peaks.

4.2.1.1 STRAIN MQ887

The genotype **isp-1(qm150)** (strain name: MQ887, see Table 3.1) for an iron-sulfur protein is involved in mitochondrial electron transport, ubiquinol to cytochrome c and positive regulation of

nematode larval development. This protein subunit is located in the mitochondrial inner membrane and respiratory chain. The qm150 is a substitution c.703G/A (or C/T on (-) strand) of the transcript F42G8.12 and a proline to serine change (P225S). Figure 4.2.1 provides the amplified area of the gene and the positions of the primers used for amplification, relative to the position of the variant. The PCR amplification of this area should theoretically result in a 1150 bp fragment, the result of which can be observed in the gel-electrophoreses analysis of the product (Figure 4.2.). The electropherogram result of the relevant area of interest, in comparison to the reference sequence, as illustrated in Figure 4.2.3, indicated the presence of the c.703C/T on the (-) strand and thus the genotype.

CAGTCCGCCCGTTGAGCATCAACTGGGGCAATGGCTTCTCTTGCTAGATCTGGAGGTTTTGCAGTCAAAG
TGATCAGCGGATCCCAGCAACATGTAAACTTTGTTGCCGCAACACCAGCCGCCGATAATGTCGCTGCTTT
CCGCGATGTTCCAGCTGAGTTCTCCACGGCTGAAGCTCGTCAAGCCGCTGTTAGTCACAGCACCGGAGGT
GTCTTCACCAATGGACTTGCTGTCAAGGGAATCAATGTCACCTCTCGCCGTTTGGCTCACACTGATGTGA
CATTCCCCGATATGTCAAACTATCGTCGTGATTCTACAAAGAACACTCAAGTGCCAGCCCGTGACACCGA
GGATCAACGTCGTGCTCTTCCAACTGCTCTGTATTATGGAGCTGGAGGAGTTCTATCTTTGTGGGCCGGA
AAGGAAGTTGTACAGACTCTTGTTTCTTACAAAGCTATGGCAGCTGATCAACGTGCCTTGGCTTCGATCG
AAATCAACATGGCTGATATTCCAGAAGGAAAAACAAAGACATTCGAATGGCGTGGAAAGCCAGTCTTCGT
CAAACATCGTACCAAGGCTGAGATTGCCAAGGAAAAGGCCGTCCCTGTCGCCGATCTCCGTCATCCACAA
CATGACGACGAACGTGTGCAGAAAGATGAATGGTCCGTTGTCATTGGAGT

c.703C/T

GTGCACCCATCTTGGATGTGTCCCAATTGCCGATGCTGGAGATTACGGAGGTTATTACTGCCCTTGTCAC
GGATCTCACTACGACGCTTCTGGACGTATTAGAAAGGGACCAGCTCCATTGAATCTTCACGTACCAGCAT
ACTCGTTCAAGGATGCCACCATCGTCATTGGATCGAGCTAAATATTCAGATTTTTTTGCAAAAGTTTCCC
CGTCCCCACTTTGAAAACTCGCGTCTCCTAATCGAATGTGTGGTTTTCTCCTGTGAAAGTAGTTGTTCCC
TTCTTTCTACGTCGTATTCTTGGCAGATAAAGTTTATTTTTCGTCCTATTTAGTGTTTGCCTGTTTTTAT
TATTTCCCCGTTTTTATCCATTTTTTCTAGGATCCCGAATGCACTCCTGTTCGAAATTCATTGCAGAATG
AATAAACGTAATTTAA**GAGGTTCTCTAGATGAGGCGGAGC**

Figure 4.1: DNA sequence of PCR amplified region of the MQ887 genotype. The forward and reverse primers are indicated in green, respectively. The yellow highlighted red letter indicates the substitution for MQ887.

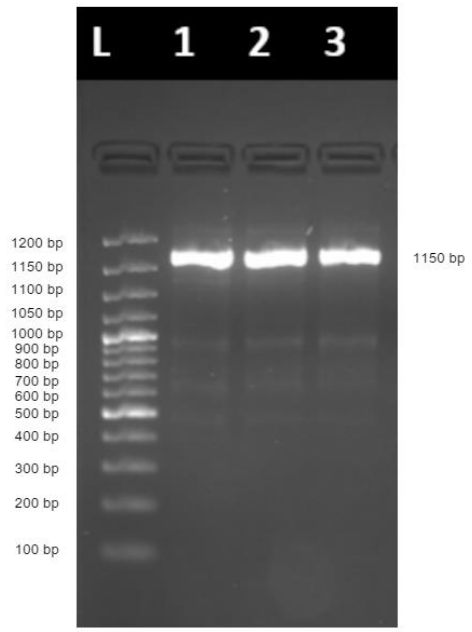

Figure 4.2. **Gel electrophoresis image indicating amplified DNA bands (~1150 bp) from the MQ887 strain.** The DNA ladder (L) in 50 bp increments is in the first lane. Lanes 1, 2 and 3 indicate three different MQ887 worms.

Figure 4.3: Electropherogram of the MQ887 sample sequence. The top strand indicates the reference (N2) sequence, and the bottom sequence the sample sequence. The red text indicates the substitution of C/T in the MQ887 strain.

4.2.1.2 STRAIN MQ1333

The genotype **nuo-6(qm200)** (strain name: MQ1333, Table 3.1) NADH Ubiquinone Oxidoreductase, located in the membrane and mitochondrion, and part of the mitochondrial respiratory chain complex I. The qm200 mutation is a substitution, c347G>A on the W01A8.4 transcripts and a Glycine to a Glutamic acid change (Gly116Glu). Figure 4.4 provides the amplified area of the gene and the positions of the primers used for amplification, relative to the position of the variant. The PCR amplification of this area should theoretically result in a 574 bp fragment, the result of which can be observed in the gel-electrophoreses analysis of the product (Figure 4.5). The electropherogram result of the relevant area of interest, in comparison to the reference sequence, as illustrated in Figure 4.6, indicated the presence of the c.347 G/C on the (-) strand and thus the correct genotype.

GGACATGAATACAATCTGAGCGACGAGGAGAAGAAAGCAGTTTTGTGGAGGTAATACGAAAAACGCTTTT
TGCTTAAAAGTTTTTAAAAAAATTCTAAAAACAGTGAGAAACATAGTTTTAATTATATTCTCAATTTAAA
ATTATTTAATTCTATTGAAAAATCAATATATGATAACATTTGCGTTGATGAACACTTATTTCAAGTGATT
TATTAGCAATAGAGACAAAAAAAAACAGTTTCTTGATATAATTTACAGAGTATCAAATCAAAAATTGCTT

TAAAAAAACTGTTGCGATAAAATTGGATATTAAACACTGAATTAACATAAATTCAGTTTTTAATATCCAA
CTTTATGATAAAAAAACTACATTTTATTTTTAAAAAATTACTTTCAGATATCGTGT

c. 347G>A

CAAGGAGATTTTGAAGAAGGAATATCTCCGTCGTGAATACGATCCTCATAGCTTCAAGTACAAGGAGGGA
GTCACCATGGATCCAGCAATGTTCCGTTGGTATTCTGCTGATATGACTCAAGCCGAGTTCTTCCGTTTCA
CACCACGC**ACCGTATTCCTGTACGTCGG**

Figure 4.4: Sequence indicating MQ1333 variant (PCR). The forward and reverse primers are indicated in green, respectively. The yellow highlighted red letter indicates the substitution for MQ1333.

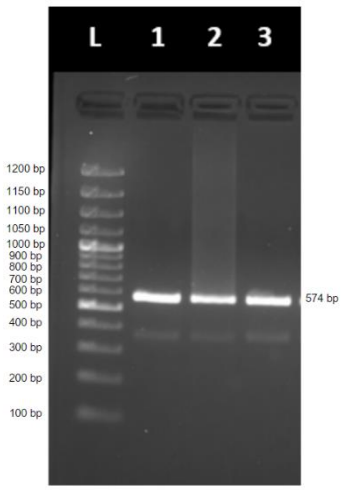

Figure 4.5: Gel electrophoresis image indicating amplified DNA (~574 bp) for the MQ1333 strain. The DNA ladder (L) in 50 bp increments in the first lane. Lanes 1, 2 and 3 indicate three different MQ1333 worms.

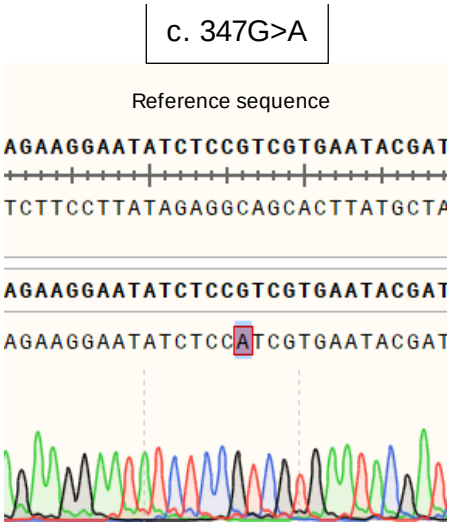

Figure 4.6: Electropherogram of the MQ1333 sample sequence. The top strand indicates the reference (N2) sequence and the bottom sequence the sample sequence. The red text indicates the substitution of G/A in the MQ1333 strain.

4.2.1.3 STRAIN LB25

The genotype **nuo-1(ua1)** (strain name: LB25, see Table 3.1) has several functions, such as ADH dehydrogenase (ubiquinone) activity; and nucleotide binding activity, inductive cell migration; and mitochondrial electron transport and NADH to ubiquinone. The mutation NADH Ubiquinone oxidoreductase is located in the mitochondria. The ua1 allele has an insertion at c.58G>T in the C09H10.3 and an Alanine to a Valine change(A352V). Figure 4.7 provides the amplified area of the gene and the positions of the primers used for amplification, relative to the position of the

variant. The PCR amplification of this area should theoretically result in a 600 bp fragment, the result of which can be observed in the gel-electrophoreses analysis of the product (Figure 4.8). The electropherogram result of the relevant area of interest, in comparison to the reference sequence, as illustrated in Figure 4.9, indicated the presence of the c.58 G/T on the (-) strand and thus the correct genotype.

c.58G>T

ACACGAATCTTGCGGACAGTGTACTCCATGCCGTGAGGGATGCAATTGGTTGAACAATATGATGTGGCGT
TTCGTTGATGGAAAAGCCAAGCCATCGGAGATCGATATGATGTGGGAACTTAGTAAACAGATCGAGGGAC
ACACTATTTGTGCTCTTGGAGACGCTGCTGCATGGCCAGTTCAGGTAAAACTATTAGTTTATTAAAAAAA
AGGAAATTTTGAACAATTATTTAGAAATAAAATTTTTAAGCTTGACGTGCAAAATATCTCGTAGCGAAAA
CTACAGTAATTCTTTGAATGACTACTGTAGCGCTTGTGTCGATTTACGGGTTCGATTTTTTGAAATTAAA
TTATTTTCGAATAGCAAGAGCTATATTTCATTTGCATTATTTTCTCATTTTCAGCTTAATTTTAATATTT
TATCGATTAATCAATTATTCCATTGAAGCCCGTATATCGACACAAGCGCTACAGTAGCCATTTTAAGAAT
TACTGTAGTTTTCGCTACGAGATATGTTGCGCAATACTTATCCTCAGAATTTTATGTTCCCGTAGTATAA
TCATTTAAAAAAATTCAAATTCCATTTCTTTG**CAGGGACTCATTCGCCA**

Figure 4.7: Sequence indicating LB25 variant (PCR). The forward and reverse primers are indicated in green, respectively. The purple letter indicates the insertion for LB25.

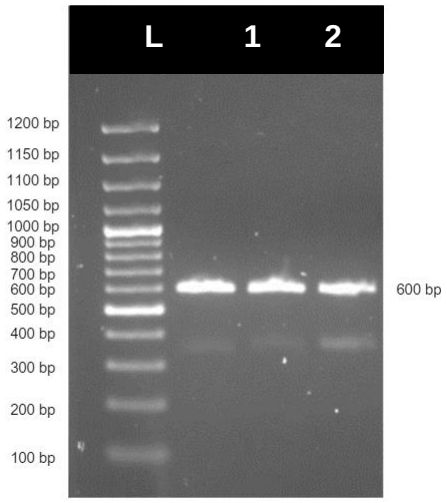

Figure 4.8: Gel electrophoresis image indicating amplified DNA (~600 bp) from the LB25 strain. The DNA ladder (L) in 50 bp increments is in the first lane. Lanes 1, 2 and 3 indicates three different LB25 worms.

Figure 4.9: Electropherogram of the LB25 sample sequence. The top strand indicates the reference (N2) sequence and the bottom sequence the sample sequence. The red text indicates the substitution for G/T in the LB25 strain.

4.2.1.4 STRAIN GA184

The genotype **sod-2(gk257)** (strain name: GA184 see Table 3.1), superoxide dismutase is involved in removal of superoxide radicals and located in the mitochondria. The gk257 allele harbours an insertion/deletion of the transcript F10D11.1. Figure 4.10 provides the amplified area of the gene and the positions of the primers used for amplification, relative to the position of the variant. The PCR amplification of this area should theoretically result in a 1050 bp fragment, the result of which can be observed in the gel-electrophoreses analysis of the product (Figure 4.11). The electropherogram result of the relevant area of interest, in comparison to the reference sequence, as illustrated in Figure 4.12, indicated the presence of the c.502ins on the (-) strand and thus the correct genotype.

AAGCACTCGCTGCCAGATTTACCATACGACTATGCTGATTTGGAGCCTGTAATCAGTCACGAGATTATGC
AACTTCATCATCAAAAGCATCATGCCACTTATGTGAACAATCTCAACCAAATTGAGGAAAAGCTTCACGA
GGCGGTCTCCAAAGGTAATTTTTTTAATTACTCAGAATTTCGGAAAGAACACTGATTGCAGGAAACGTCA
AAGAAGCTATCGCTCTTCAGCCAGCTCTCAAGTTCAATGGAGGAGGACATATCAACCACTCCATCTTCTG
GACTAATTTGGCAAAGGACGGAGGAGAACCATCGGCGGAGTTGCTCACCGCAATTAAGGTAGTTTATTAG
TCATATCAGGCAGTCAATAATAATACTTAAAGTTAAAAGTCGATATTAAAAATGTAGTGAACACGATTTG
TGCGGTCAAGGCTGAGATTAAAATGATTCAACGTTTTAGAATTTTGTATAATCG

c.502ins TTATATTTGACTATTTGA

GCTTAGCCTTTACAGTATTTTGATT**TTATATTTGACTATTTGA**ATTGATATTTAATTCGCATTGAACAAC
TCTAGCACTGGCCATTGTTCAATTTAAAACATTTTCAGAGCGACTTCGGATCTCTGGATAATCTTCAAAA
ACAGCTTTCGGCATCAACTGTCGCTGTTCAAGGATCAGGATGGGGATGGTTGGGATACTGTCCAAAGGGA
AAGATCTTGAAGGTTGCCACATGTGCCAATCAGGATCCACTTGAGGCAACAACTGGACTTGTTCCACTGT
TCGGAATTGACGTCTGGGAGCACGCTTACTACTTGCAGTACAAGAATGTTCGACCAGATTATGTCAATGC
TATTTGGAAGGTAGTTGTCACTTTCCATCAAAATTAATATTTTTAATTTAAAATCTTTCAGATCGCCAAC
TGGAAGAACGTCAGCGAGCGTTTTGCAAAGGCACAGCAATAAATGAGCTGAATCACAAGAATTAATCGTC
AAATGTAGCAGTAGAAGTTGACTCCCATTGTTTTGTAACTATTTTTGTTTCTTAATTATTTCGAAATGTA
AATTTTCAAACCTTTTCAA**ATGAAAAGTTTTCACCG**

Figure 4.10: Sequence indicating GA184 variant (PCR). The forward and reverse primers are indicated in green, respectively. The purple letters indicate the insertion for GA184.

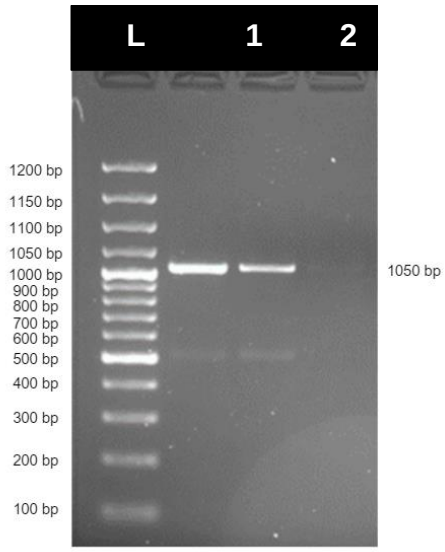

Figure 4.11: Gel electrophoresis image indicating amplified DNA (~1050 bp) from the GA184 strain. The DNA ladder (L) in 50 bp increments is in the first lane. Lanes 1, 2 and 3 indicate three different GA184 worms.

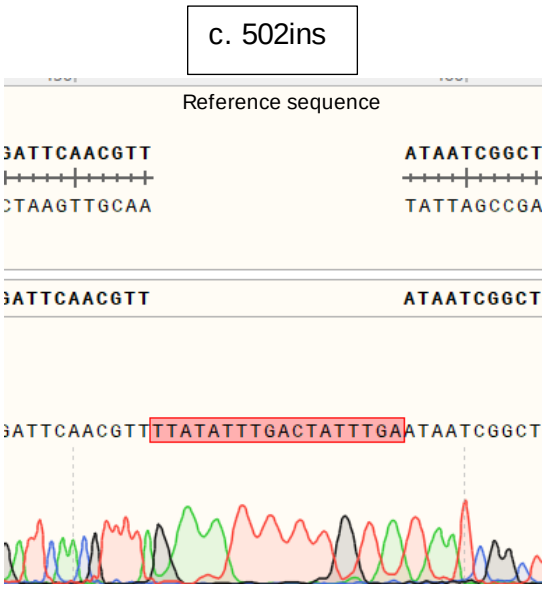

Figure 4.12: Electropherogram of the GA184 sample sequence. The top strand indicates the reference (N2) sequence and the bottom sequence the sample sequence. The red text indicates the insertion in the GA184 strain.

4.2.1.5 STRAIN CW152

The genotype **gas-1(fc21)** (strain name: CW152, see Table 3.1) is General Anesthetic Sensitivity abnormal and is involved in mitochondrial electron transport, NADH to ubiquinone and response to drug located in the intracellular membrane-bounded organelle. The fc21 is a substitution c.451G>A on the PCR product of the K09A9.5 transcripts and an Arginine to a Lysine change (R290K). Figure 4.13 provides the amplified area of the gene and the positions of the primers used for amplification, relative to the position of the variant. The PCR amplification of this area should theoretically result in a 600 bp fragment, the result of which can be observed in the gel electrophoreses analysis of the product (Figure 4.14). The electropherogram result of the relevant area of interest, in comparison to the reference sequence, as illustrated in Figure 4.2.15, indicated the presence of the c.415 G/A on the (-) strand and thus the correct genotype.

ATCGTCTCGATTACGTCTCCATGATGTGCAATGAGCAGGCTTGGTCTTTGGCTGTTGAGAAGCTTCTCGG
TATTGACATCCCAACAAGAGCCAAATATATCAGAACTCTCATGGGAGAGCTCACTCGCATCCAGAACCAC
ATCATGGGTATCACCACTCACGCCCTTGACGTTGGAGCTATGACACCGTTTTTCTGGATGTTCGAGGGTA

AGTTTATTGTTTCAAAATAAGTACAAAACCAACATTGATTTTCAGAACGTGAAAAGCTCTTTGAGTTTTC
CGAGCGAGTATCTGGTGCCAGAATGCATGCCAACTACGTCCGCCCCGGAGGTGTCGCTTGGGATCTTCCA
ATTGGTCTTATGGATGACATCTACGACTGGGCCATCAAGTTCCCAGAACGTATCGA

c.451G>A

TGAGCTCGAAGACATGCTCACCGAAAACCGAATCTGGAAGGCCAGAACTATTGACATCGGACTTGTGTCA
GCTGCTGATGCTCTCAACTGGGGATTCAGTGGAGTCATGGTCCGTGGATCTGGAATCAAGCAAGACGTGA
GAAAGACCGAACCATACGATGCCTATGCTGATATGGAATTTGATGTTCCAATCGGAACCAAGGGTGATTG
CTACGACAGATA**CTTGTGCCGTATTGAGGAGAT**

Figure 4.13: Sequence indicating CW152 variant (PCR). The forward and reverse primers are indicated in green, respectively. The yellow highlighted red letter indicates the substitution for CW152.

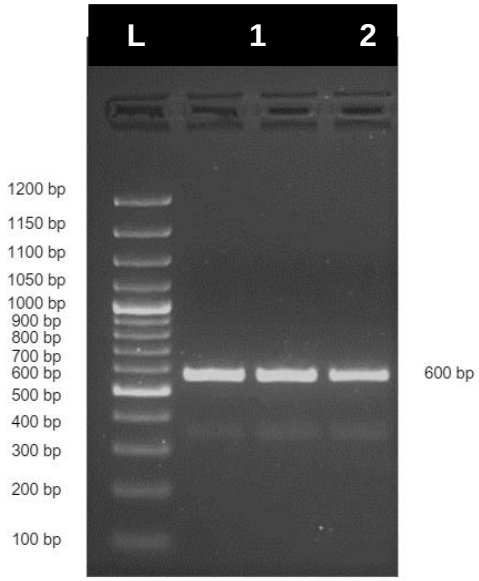

Figure 4.14: Gel electrophoresis image indicating amplified DNA (~600 bp) from the CW152 strain. The DNA ladder (L) in 50 bp increments in the first lane. Lanes 1, 2 and 3 indicate three different CW152 worms

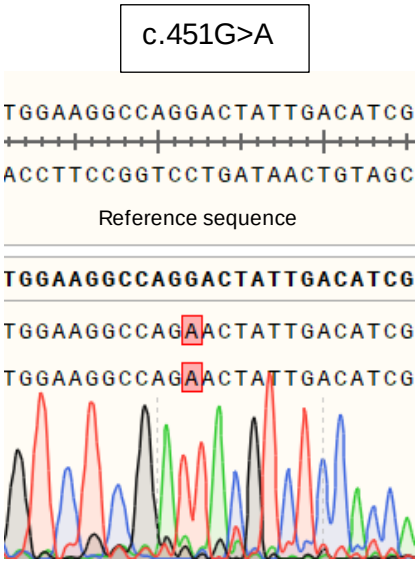

Figure 4.15: Electropherogram of the CW152 sample sequence. The top strand indicates the reference (N2) sequence and the bottom sequence the sample sequence. The red text indicates the substitution for G/A in the CW152 strain.

4.2.1.6 STRAIN TK22

The genotype **mev-1(kn1)** (strain name: TK22, see Table 3.1) is abnormal MEthyl Viologen sensitivity and is predicted to be involved in the defense response to other organism;

mitochondrial electron transport, succinate to ubiquinone; and regulation of the response to oxidative stress and is located in the mitochondria. The kn1 mutation has a G>A substitution at 212 bp and shows a Glycine to Glutamic acid change (G71E) on the T07C4.7a.1. Figure 4.2.16 provides the amplified area of the gene and the positions of the primers used for amplification, relative to the position of the variant. The PCR amplification of this area should theoretically result in a 400 bp fragment, the result of which can be observed in the gelelectrophoreses analysis of the product (Figure 4.17). The electropherogram result of the relevant area of interest, in comparison to the reference sequence, as illustrated in Figure 4.18, indicated the presence of the c.212 G/A on the (-) strand and thus the genotype.

TTCCAACTGCGATTCTGTGCCGCTTGGGCGCCAGATCGTCGATTTCCCGCTCCTTTGGAACATCGATCGT
CACCAAGGTGGGGATTTTTTGAATTTTTCCGTGAAAATTGTTGATTTTTTGTGTACGCATGAAGGAGAAA
TGTATAACAGACACATTCTTTTCAATTAATTATTTATAATATTCACAGTCCGAGGCAAAGACGCCAATCC
AGAAGTTCGGATGGGAATACCTGTTGAAGCAGCGCTCCAAGAATCGCCCAATCGCTCCAC

c.212G>A

ATCTCACCGTCTACCAGCCACAATTGACCTGGATGCTCTCCGAATTCCATAGAATCAGCGGTTGTGTAAT
GGCCGGAACCCTTCTCGTCGGAGGAATCGGATTCGCAGTTT**TGCCGTTCGATTTCACCGC**

Figure 4.16: Sequence indicating TK22 variant (PCR). The forward and reverse primers are indicated in green, respectively. The yellow highlighted red letter indicates the substitution for T522.

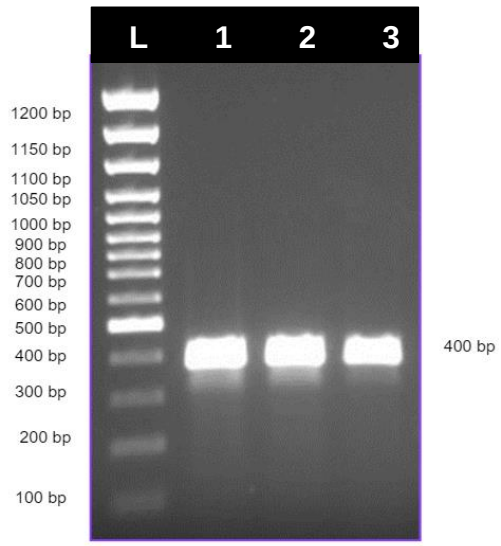

Figure 4.17: Gel electrophoresis image indicating amplified DNA (~400 bp) from the TK22 strain. The DNA ladder (L) in 100 bp increments in the first lane. Lanes 1, 2 and 3 indicates three different TK22 worms.

Figure 4.18: Electropherogram of the TK22 sample sequence. The top strand indicates the reference (N2) sequence and the bottom sequence the sample sequence. The red text indicates the substitution for G/A in the TK22 strain.

4.2.2 GENOTYPING DISCUSSION

Prior to the commencement of this study, the first step was to confirm the reported genotype of the strains received from CGC. This was PCR amplified, and the Sanger sequencing of specific DNA segments of the mutant strains using specific designed primers for each genotype (WormBase, 2022). The data processing included alignment, followed by comparisons of the test genotype sequences to the reference sequence in the areas where the deletions or substitutions for the respective genotypes were expected. The known variations were all identified and confirmed as correct genotypes for downstream analyses.

4.3 OXYGEN CONSUMPTION RATES

After confirming the genotypes of the strains, mitochondrial function was evaluated by measuring the basal OCR using the Oroboros O2K Flux Analyzer. Previous reports indicated that nematodes of selected mutants display a significant reduction in oxygen consumption (Hench *et al*., 2011).

Thus, this study sought to measure OCRs of all mutants and N2 wild-type adults. They used L4 adults due to the small quantity and insufficient nematodes on the plate of L1 and L2 nematodes. Importantly, optimisation of nematode numbers had to be done prior to the actual analysis to ensure accurate estimation of OCRs.

4.3.1 OPTIMISING NUMBER OF WORMS THAT ARE NEEDED FOR ANALYSIS

OCR optimisation was done to assess an optimal number of worms needed for measuring before final OCR could be done on the strains. The results summarised in Fig 4.3.1 show the concentration range of the 100 to 500 worms that were analysed (n = 4). The flux was obtained from the DatLab software. All runs were ±25 minutes and the flux are measured as $pmol \cdot s^{-1} \cdot ml^{-1}$. The average specific flux wasc calculated from the four measurements per number of worms. Fig 4.3.2 shows the specific flux per worm. From the results, it is observed that a near linear increase in OCR occurred with an increase in the numbers of worms over this range. It is also observed that the flux response would be similar over this range, but since picking worms is time consuming and a potential limiting factor in the process, a lower number of worms would be ideal – if a well detectable flux response can be measured (which is the case in the range). Thus, a near linear relationship was observed between the average OCR and the number of worms between 200 and 500. In additional analyses (results not shown), it was also determined that the reliable detection limit, from which to distinguish the background consumption, was 50 worms.

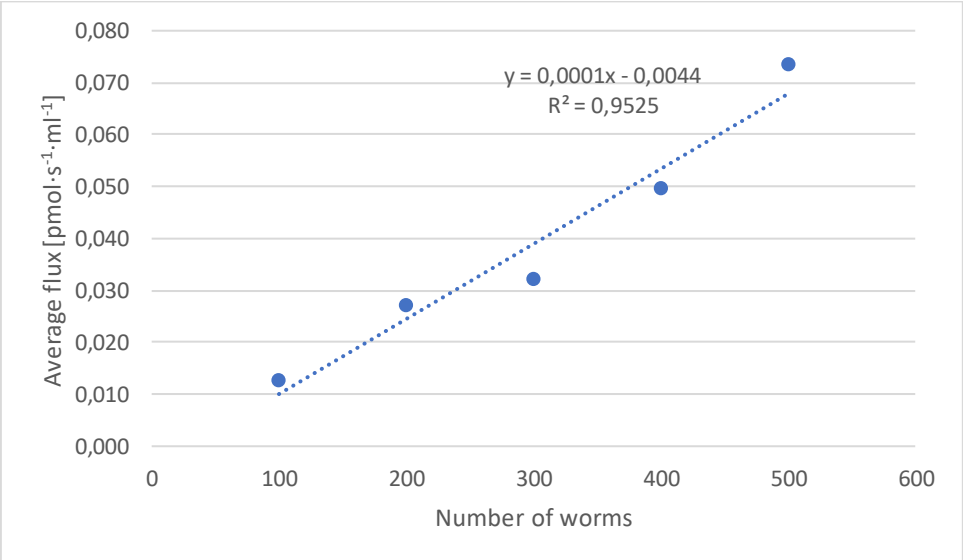

Figure 4.3.1: Average flux of concentration range of nematodes. The average specific flux ($P<0.05$) in comparison to the number of worms.

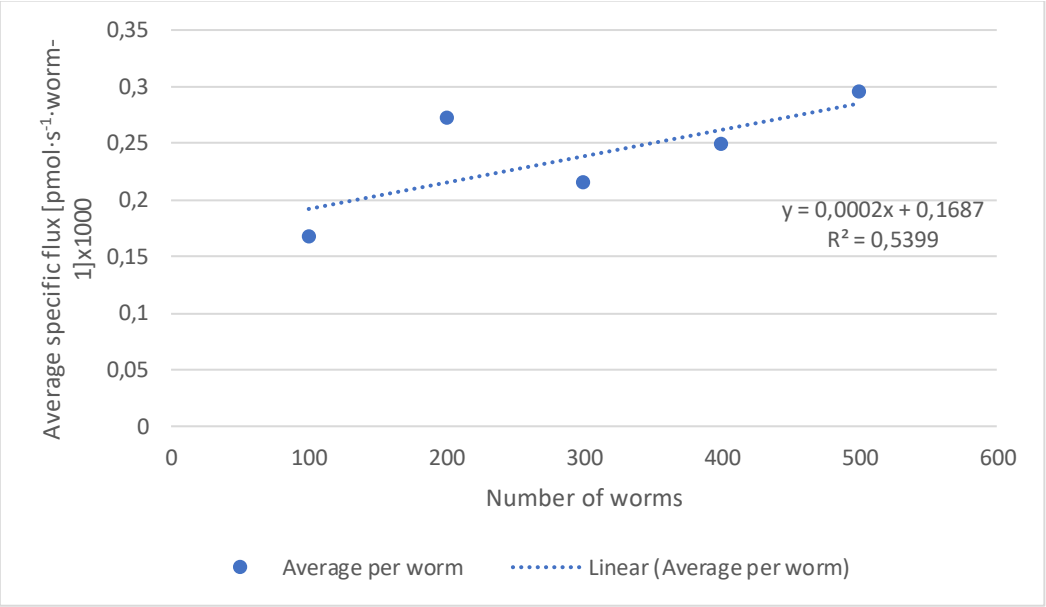

Figure 4.3.2: Average specific flux per worm. The average specific flux per worm. For the OCR, 200 worms were chosen for the analysis because it falls within the curve, and it is a realistic and achievable quantity of worms to collect ($P<0.05$).

4.3.2 RESULTS OF OXYGEN CONSUMPTION RATE ANALYSES IN STRAINS

The basal respiration rate was determined using OROBOROS Oxygraph 2K adapted from Taferner *et al.*, 2015. Approximately 200 worms were collected in M9 buffer, washed, and delivered to the chamber in 2.5 ml M9 buffer. The respiration was normalised to the number of worms to give specific flux with DatLab. Initial baseline consumption and stabilisation of the Oxygraph was done before adding the nematodes. Nematodes were then added and given ±5 min to recover before OCR was measured; after this, the next 15–25 min were used for the analysis of OCR. As an example of a result for these analyses, Fig 4.3.3 shows a typical oxygen trace where the stable redline indicates the O_2 consumption rate (red line, slope negative) and a resulting decrease in O_2 concentration (blue line).

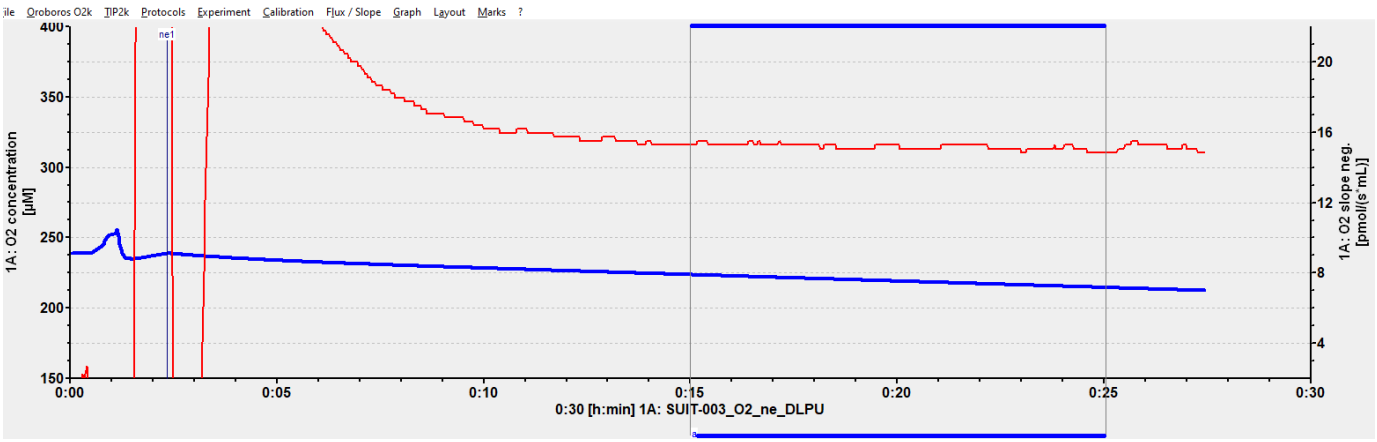

Figure 4.3.3. Example of high-resolution respirometry trace as performed in an Oroboros Oxygraph 2k. The blue line shows the oxygen concentration in the sealed chamber and the red line shows the OCR of the nematodes. At 5 min, the chamber was opened, and nematodes were added; then ± 5 min given to recover. Analyses time was consistently 15-25 min.

After completion of all the Oroboros runs, the data points were collected and analysed. As indicated before, 200 worms were used for all strains in the volume used after successful optimisation, and the results, as shown in Fig 4.3.4, are expressed as average flux per volume [pmol·s^{-1}·mL^{-1}] (n = 4). For the wild-type N2, an average of 19 [pmol·s-1·mL-1] was determined and used in comparison to the knockout strains. Compared to N2, as can be observed in Fig 4.3.4, except for the LB25 and MQ887 mutants, all other mutants show a significant decrease compared to the wild type, with the positive control for inhibition (N2-treated with rotenone) the lowest. From the results, compared to untreated N2, in the order of highest to lowest, the strains that showed significant reduction in OCR were MQ133 (60.3% relative to N2), GA184 (60.0%), TK22 (48.3%), and CW152 (31.4%). Furthermore, the values were used as per volume. The LB25 (7.2%) and MQ887 (16.9%) mutants did not show a significant decrease in OCR (P>0.05).

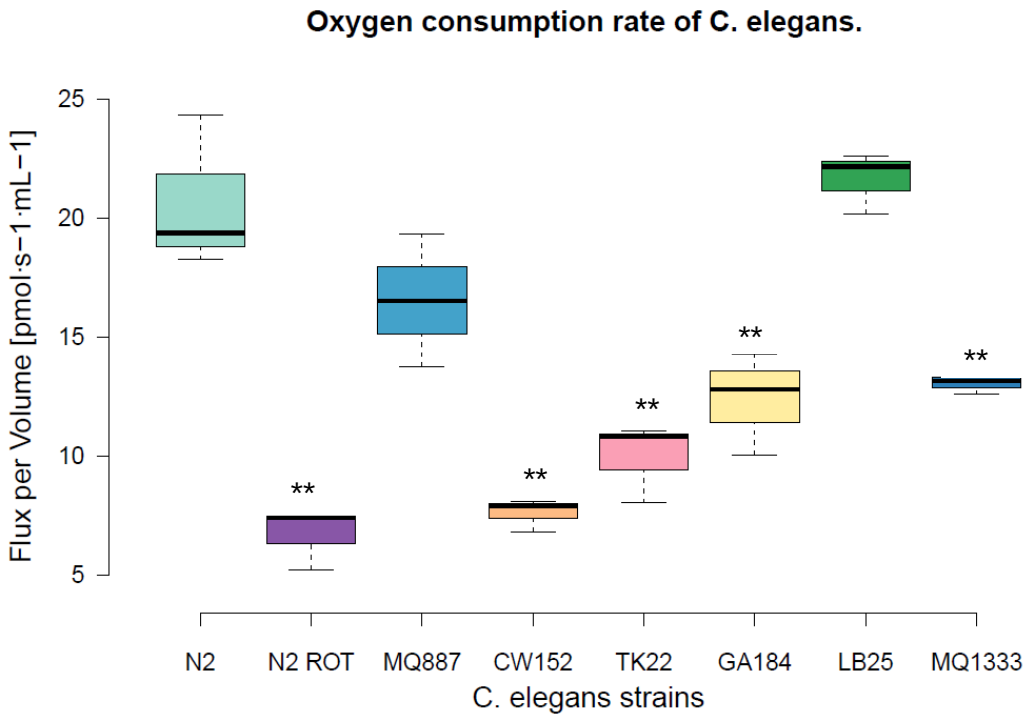

Figure 4.3.4: Boxplot depicting the OCR of all strains. The average OCR of *C. elegans* was determined by Oxygraph 2K measurements and the basic respiration rate was determined. N2 and N2 (treated with Rotenone as a control) showed a significant difference (P<0.05). Compared to wild type, the CW152, TK22, GA184 and MQ1333 of the OCR was significantly decreased (** denotes P<0.05 as compared to the wild type).

4.3.3 DISCUSSION

C. elegans intestinal cells are highly metabolic cells with heavy mitochondrial demands (Burnell *et al*., 2005). OCR provides an indirect method to evaluate the energy metabolism of mitochondria. Therefore, mitochondria in these cells may generate large amounts of ROS, if inhibited. Following the OCR analysis, some of the KO mutants (CW152, TK22, GA184 and MQ1333) showed a significant decrease in OCR. The precise mechanisms of decreased mitochondrial OCR have not been investigated in this assay, but considering the mechanisms as reviewed before, it can be inferred that the various enzyme deficiencies of the mutants, as described below, can be associated with reduction of OCR. The mutants that showed a decrease in OCR do relate to the expected outcomes because a KO of any of the genes related to OXPHOS may contribute to a decrease in the mitochondrial function.

The OCR of CI (CW152 & MQ1333), CII (TK22) and *sod-2* (GA184) were significantly decreased ($P<0.05$) and more than 30% decreased, which may indicate that overall mitochondrial function is affected and plays a crucial role in ETC during oxidative phosphorylation. The increased ROS may be of electron leakage, mitochondrial dysfunction CI and CIII contribution. Most of the data points were tightly clustered with relatively low STDEV, which is a good indication of reproducibility. The CI components, which are NADH:ubiquinone oxidoreductase and CII, may have been disrupted, which led to an accumulation of electron carriers in the ETC. This may contribute to increased ROS and oxidative stress. Consequently, the electrochemical gradient that is required for ATP synthesis is disrupted and eventually leads to diminished cellular energy levels. Cells may then try to compensate to restore energy production and these mechanisms could involve upregulation of other metabolic pathways, such as glycolysis, to maintain ATP levels and cellular viability. Techniques such as mitochondrial respiration measurements or pharmacological interventions are possible procedures to elucidate the specific mechanisms that are involved in the observed decrease in OCR. The CIII KO, MQ887, did not show a significant decrease in OCR ($P>0.1$). A possible mechanism for the unchanged OCR is overcompensation from CI and CII to reduce electron carriers so that ATP synthesis can still proceed.

4.4 PHENOTYPIC EVALUATIONS

Since mitochondrial defects in humans and animals are linked to a plethora of phenotypic changes, mostly affecting tissues that are most energy demanding, the movement (locomotion behavior) of the nematodes were compared between the different mutants and the wild-type N2. Analyzing the locomotion behavior conceivably requires muscle and mitochondrial function. Understanding the behavioral control of the worms' locomotion is important for understanding of many more complicated behaviors. The movement of nematodes were counted as body bends during one-minute intervals. Previous studies have shown a significant decrease in locomotion behavior in some of the mutants included in this study, compared to wild-type (Lavorato *et al*., 2021). Figure 4.4.1 provides the comparative locomotor behavior between the strains used.

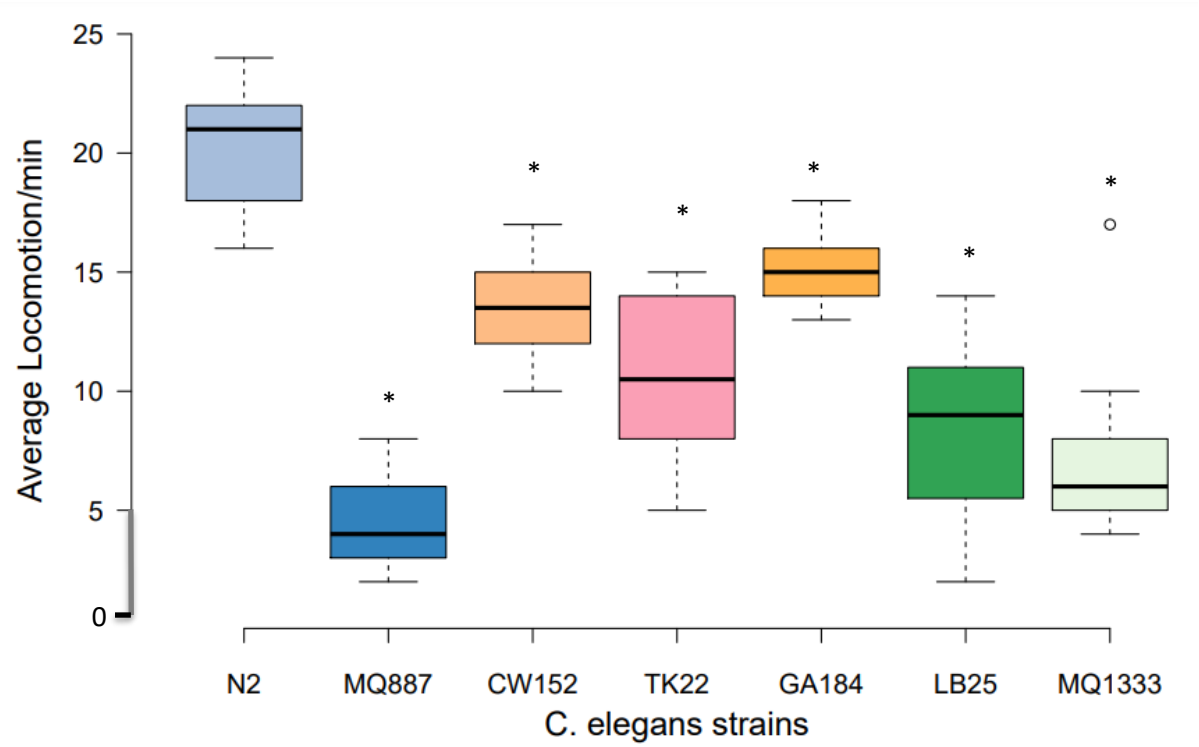

Figure 4.4.1 Locomotion of *C. elegans* strains. The average number of movements (sigmodal/body bends) per minute (Y-axis) of all the strains (X-axis) compared to the wild-type is illustrated. For each strain 30 worms were analysed. (N = 30, * P<0.05).

DISCUSSION

Compared with wild-type worms, which moved forward for a long duration, some mutants only moved forward for a short duration before reversing and turning. The nematodes changes in movement were dramatically impaired in their ability to move forward for long distances. Within seconds of placing N2 worms on agar, the worms began to move. Within 1 min of recovery the worms were already moving forward. Mutant worms on the other hand, some of the worms took more than 30 seconds to start moving after placed on the agar. All the mutant strains showed a significant decrease in locomotion compared to the wild-type P<0.05. The order of most to least affected strains were as follows: MQ887>MQ1333>LB25>TK22>CW152>GA184>N2, with MQ887 being ~18% of the movement in N2.

4.5 MEASUREMENT OF ROS IN *C. ELEGANS*

As its title implies, this study was undertaken to evaluate *C. elegans* models with OXPHOS deficiency and their ROS levels. To analyse ROS production in the mitochondria of the nematodes, we conducted a MitoSOX assay using fluorescence microscopy – which also provided a qualitative/visual estimation of ROS formation. MitoSOX is a fluorescent dye that selectively binds to superoxides in the mitochondria. Worms were exposed to MitoSOX using a modified protocol, as previously described by Zhang *et al*., 2021. Days 4-5 of the worms were chosen to represent the midlife of the worms, where disease symptoms may begin to manifest. Nematodes were incubated in MitoSOX for ± 4 hours in M9 media. After this treatment, nematodes were incubated with the irreversible inhibitor of CI, rotenone, which results in increased ROS production. This latter step was included as a positive control for ROS production (Heo *et al*., 2022). Nematodes without any probe or inhibitor were also imaged to make sure no ROS or auto fluorescence were detected (not shown). To successfully target mitochondria, the MitoTracker was first used in conjunction with MitoSOX to confirm the site and that the ROS detected is indeed mitochondrial ROS.

MITOCHONDRIAL ROS

Before the final ROS measurements were done, it was relevant to this study and the comparison of the various nematode strains to confirm that the majority of ROS that was measured was indeed mitochondrial ROS, and that the procedure of generating the data was qualitatively convincing. Therefore, MitoTracker was used to localise mitochondria in cells all over *C. elegans* to ensure mitochondrial ROS was measured. Figure 4.5.1 shows a wild-type *C. elegans* and the localisation of superoxides. The analysis confirmed that superoxide indeed localises with mitochondria, whereas not all mitochondria in the pharyngeal bulb area produce superoxide, as can be observed from areas remaining green in Figure 4.5.2C. After confirming co-localisation of superoxide ROS with mitochondria, the ROS measurements were done for all nematode strains, using the pharyngeal bulbs area as further illustrated in Figures 4.5.3-9. Figures 4.5.10 and 4.5.11 summarise the quantified results of the mitochondria ROS in all the strains without (4.5.10) and with (4.5.11) the addition of rotenone.

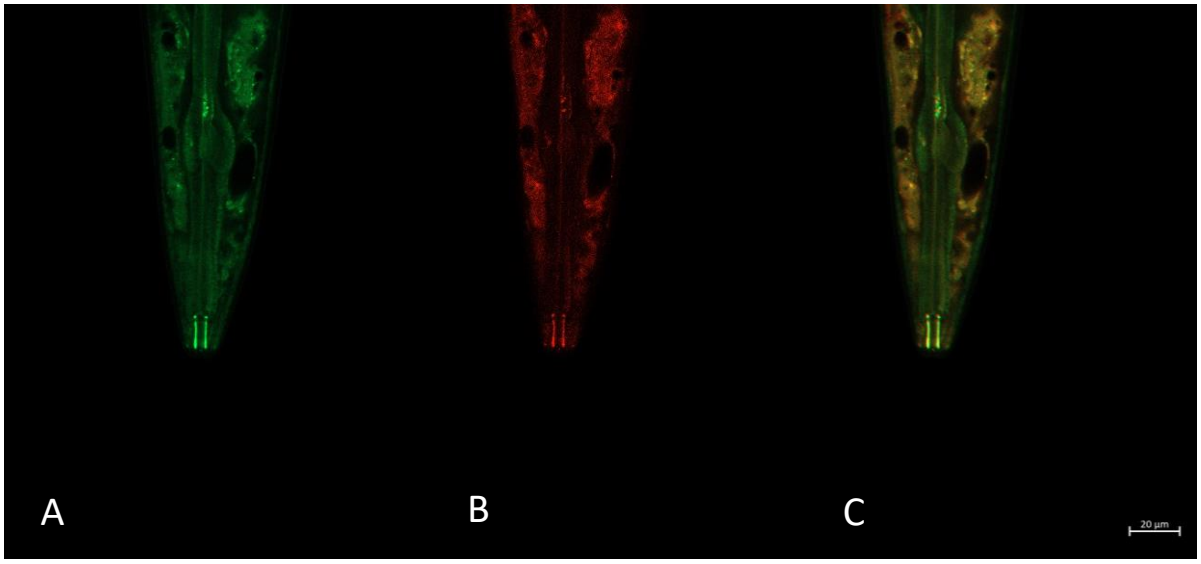

Figure 4.5.1 Co-localisation analysis of mitochondria and superoxide ROS in *C. elegans*. An overlay of MitoTracker and MitoSox fluorescent image in N2 *C. elegans*. (A) shows a nematode with MitoTracker (green), highlighting mitochondria, while (B) shows MitoSox (red), that targets superoxide ROS. (C) shows an overlap of the two images to confirm the co-localised ROS within the mitochondria. Scale bar indicates 20 µm.

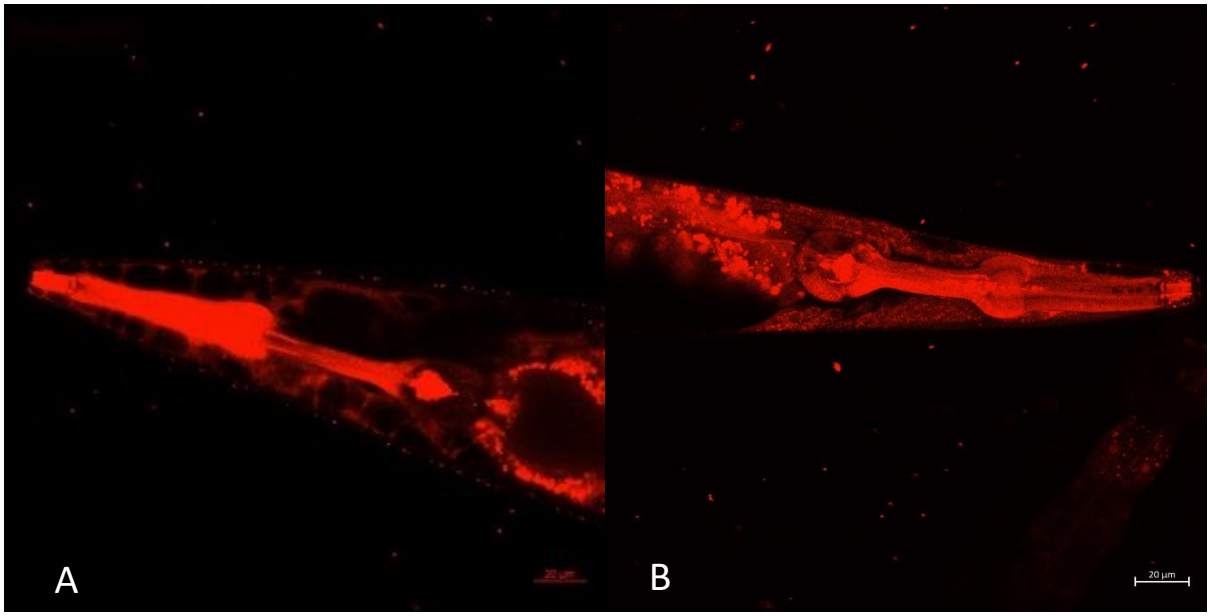

Figure 4.5.2. ROS measurement of CW152. Representative image of the CW152 strain during live ROS measurement treated with MitoSOX. (A) shows CW152 treated with MitoSOX while (B) shows CW152 treated with Rotenone and MitoSOX. Scale bar indicates 20 µm. Each image was

individually analysed qualitatively and quantitatively using ImageJ and fluorescent intensities. To obtain corrected fluorescent intensities, the background noise was subtracted from all images that follow.

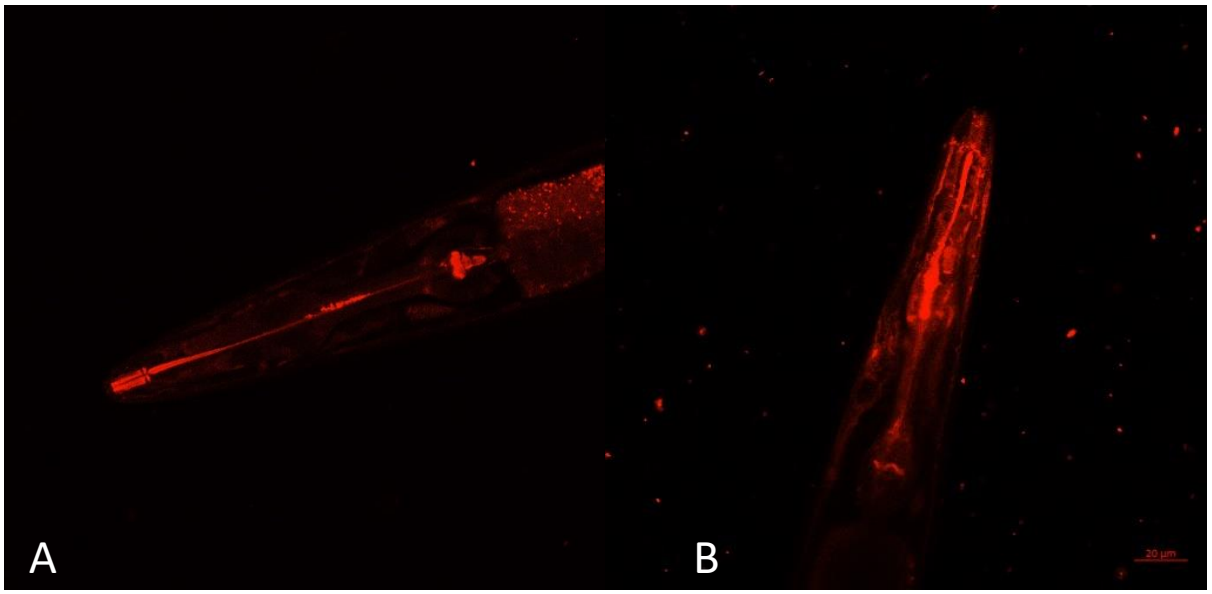

Fig 4.5.3. ROS measurement of LB25. Image of the LB25 strain during live ROS measurement treated with MitoSOX. (A) shows LB25 treated with MitoSOX while (B) shows LB25 treated with Rotenone and MitoSOX. Scale bar indicates 20 µm.

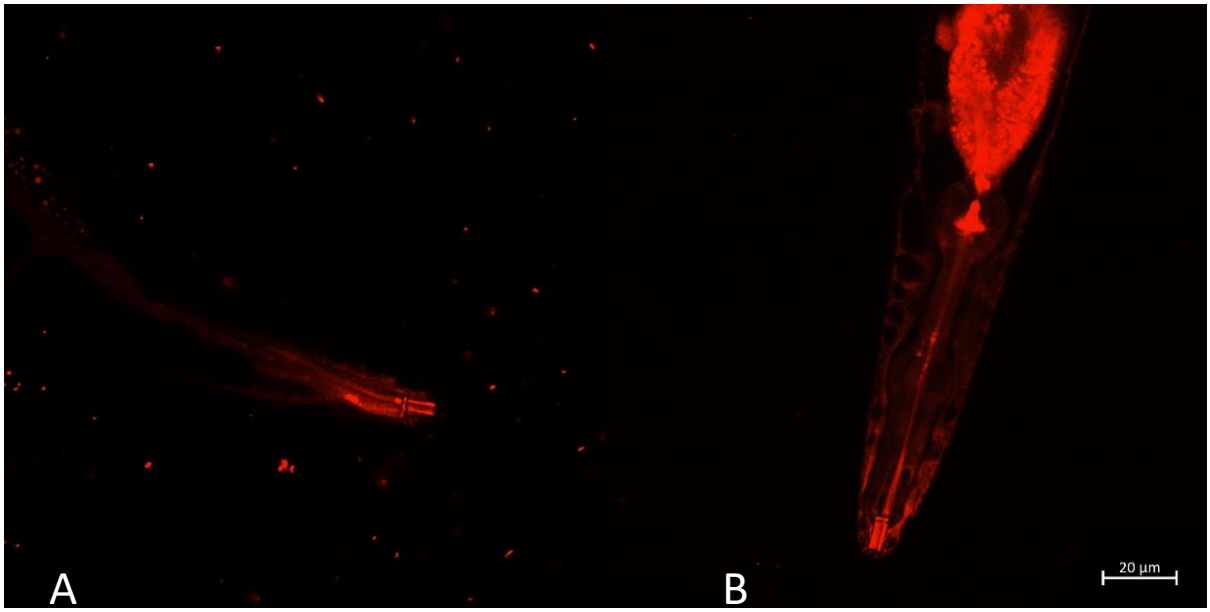

Fig 4.5.6. ROS measurement of MQ887. Image of the MQ887 strain during live ROS measurement treated with MitoSOX. (A) shows MQ887 treated with MitoSOX. (B) shows MQ887 treated with Rotenone and MitoSOX.

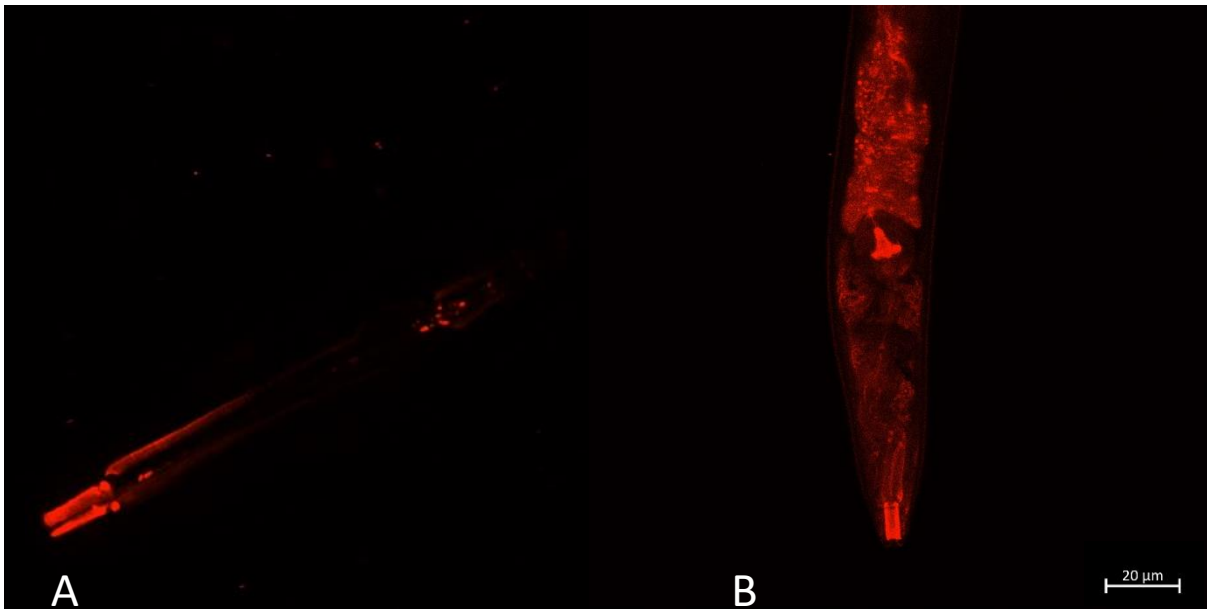

Fig 4.5.7. ROS measurement of MQ1333. Image of the MQ1333 strain during live ROS measurement treated with MitoSOX. (A) shows MQ1333 treated with MitoSOX while (B) shows MQ1333 treated with Rotenone and MitoSOX. Scale bar indicates 20 µm.

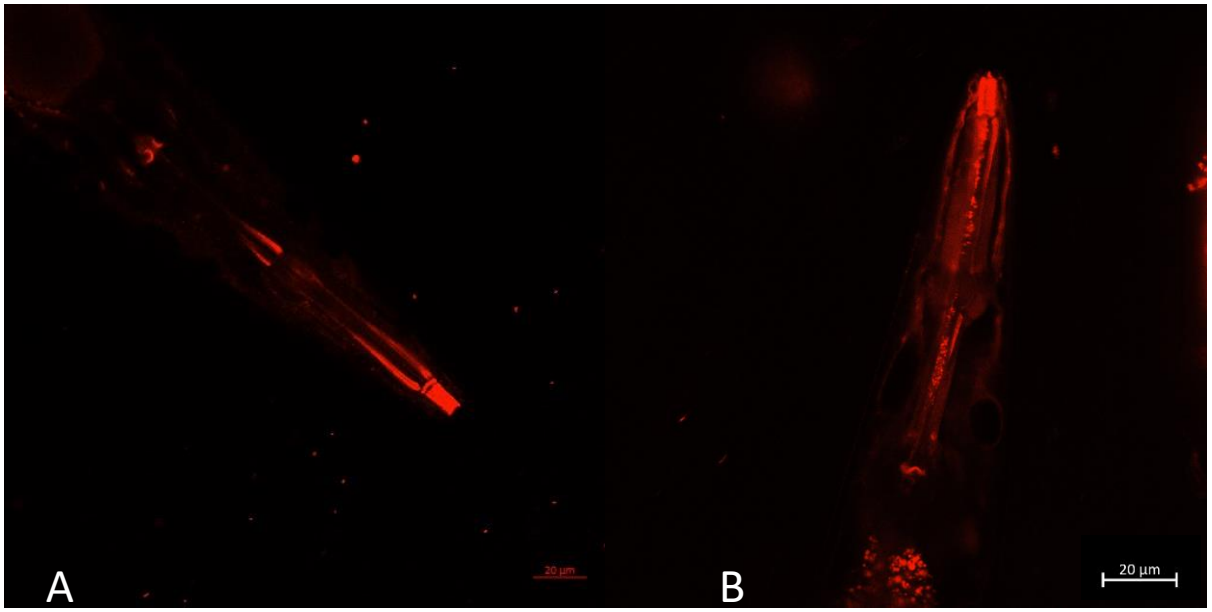

Fig 4.5.8. ROS measurement of GA184. Image of the GA184 strain during live ROS measurement treated with MitoSOX. (A) shows GA184 treated with MitoSOX while (B) shows GA184 treated with Rotenone and MitoSOX. Scale bar indicates 20 µm.

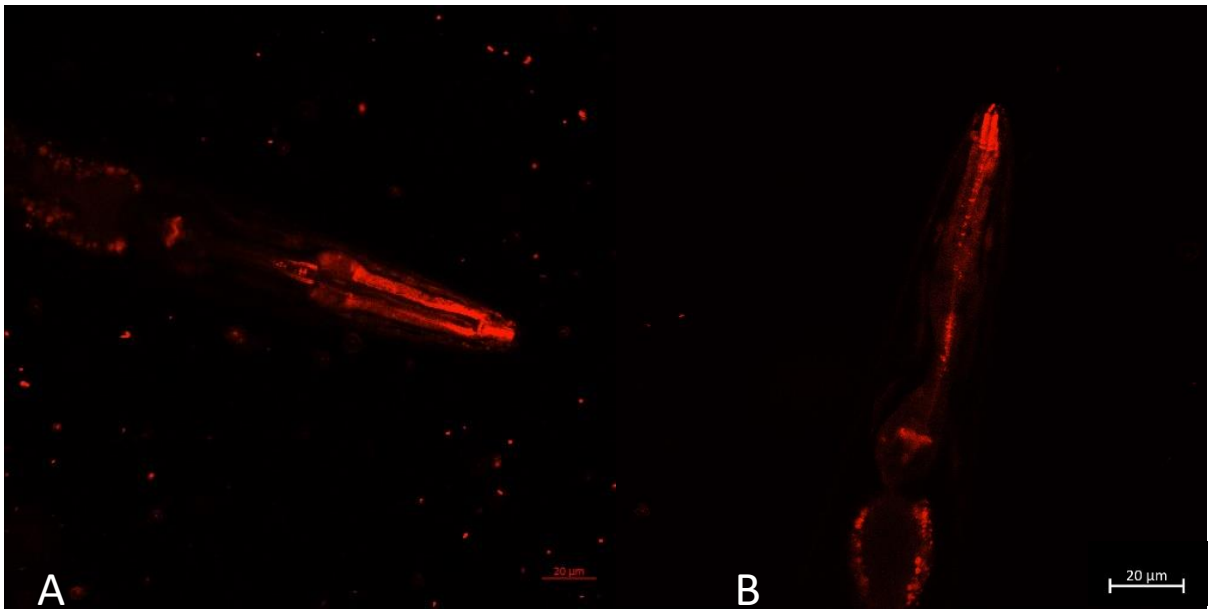

Fig 4.5.9. ROS measurement of TK22. Image of the TK22 strain during live ROS measurement treated with MitoSOX. (A) shows TK22 treated with MitoSOX while (B) shows TK22 treated with Rotenone and MitoSOX. Scale bar indicates 20 µm.

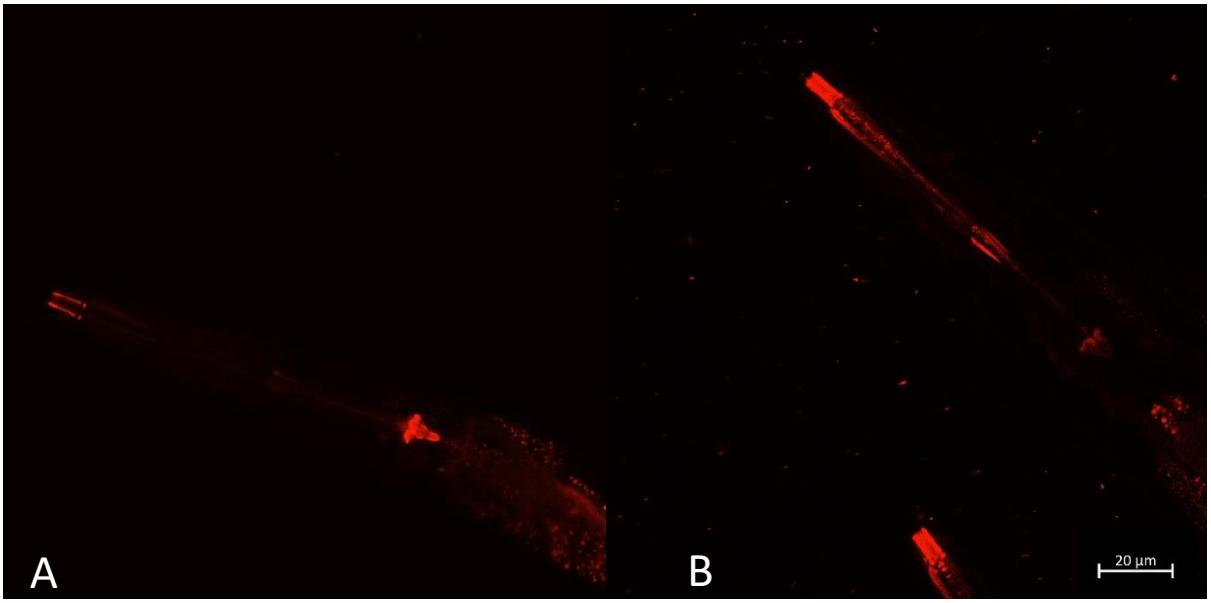

Fig 4.5.9. ROS measurement of N2. Image of the N2 strain during live ROS measurement treated with MitoSOX. (A) shows N2 treated with MitoSOX. (B) shows N2 treated with Rotenone and MitoSOX. Scale bar indicates 20 µm.

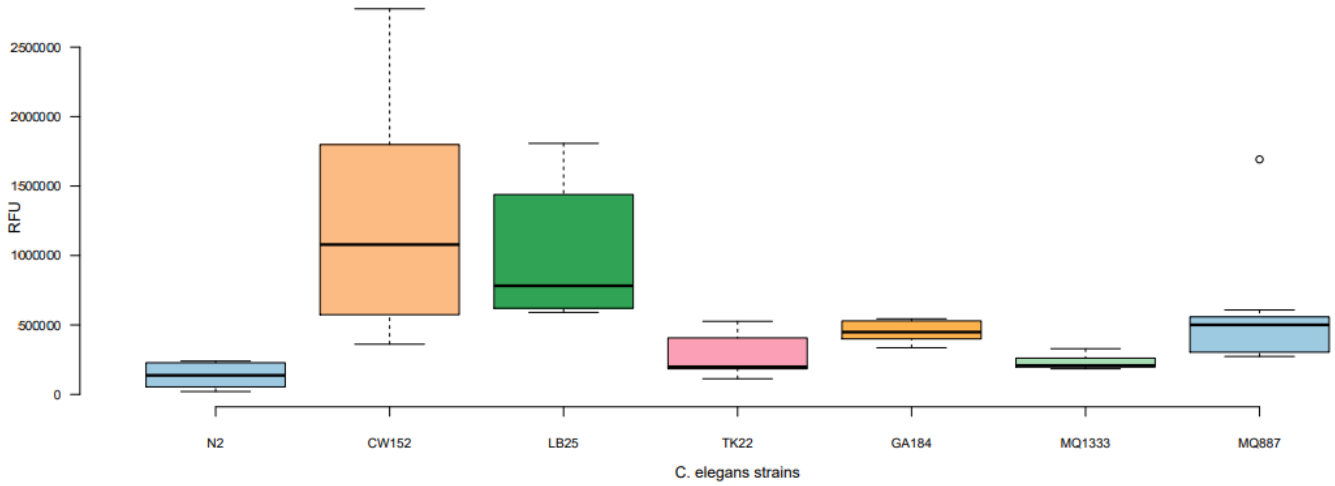

Figure 4.5.10. Mitochondrial ROS of *C. elegans* mutants.

The fluorescence intensities displayed as a measurement of ROS in *C. elegans* using MitoSOX represented as a boxplot. Relative fluorescence units (RFU) plotted on the Y-axis against the mutant strains compared to the WT (N2) on X-axis. Each strain was analysed and a minimum of n=6 worms were measured; the average was then used in the boxplot, with upper and lower values indicated with the limits of the box and the average being the dark line in the middle of the box (STDEV indicated as whiskers).

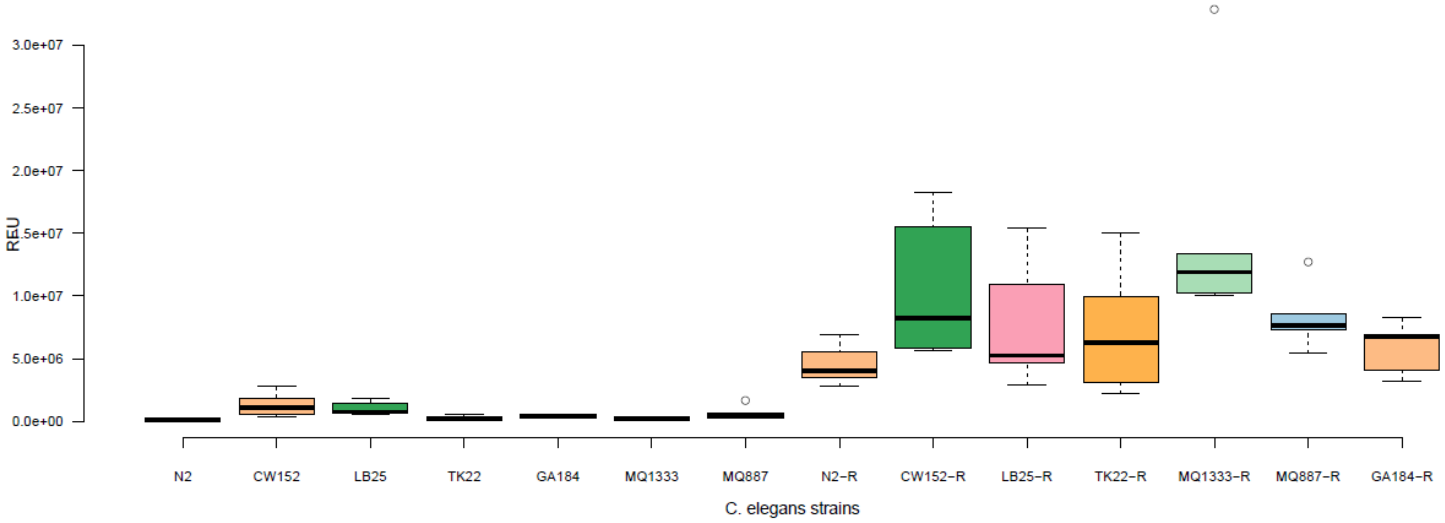

Figure 4.5.11 Mitochondrial ROS of rotenone-treated *C. elegans* mutants.

This figure depicts the difference between a mutant and a treated mutant with rotenone to induce excessive ROS. Firstly, the seven normal strains with MitoSOX (and no rotenone to give perspective) and secondly, denoted with R, are the seven strains that were treated with rotenone and MitoSOX. Relative fluorescence units (Y-axis) against the mutant strains on X-axis.

4.6 DISCUSSION

Comparing each strain with strain treated with rotenone (N2 v N2-R) shows significant difference for all strains (P<0.05). Comparing mutant strains treated with rotenone to the wild type (MQ887-R v N2), all showed a significant increase in ROS (P<0.05). When comparing all the mutant strains (not treated) to the wild type, all the strains showed a significant increase in ROS levels (P<0.05), except for TK22 and MQ1333, which was not significant (P>0.05). It was evident that some of these mutants (notably CW152 and LB25) have, compared to others, shown a more significant increase in ROS. The order in relative increase in ROS was CW152>LB52>MQ887>GA184>MQ1333>TK2>N2, with CW152 exhibiting a ~937% higher level of ROS compared to N2. The relative increase in ROS when treating with rotenone did not give the same order of relative ROS increase compared to untreated worms, which was in the order MQ1333>CW152>MQ887>GA184>TK2>LB52>N2, with MQ1113 ~245% higher than rotenone treated N2. The GA184 (SOD) was utilized to discern how the absence of this antioxidant enzyme impacted various cellular processes or responses compared to the wild-type or other stains. Comparing GA184 to the wild-type also showed a significant increase in ROS (P<0.05) which indicates a functioning secondary control in this study. Such increase ROS levels in GA184, in

relation to the wild-type, indicate a distinct oxidative shift or irregularity within the cellular environment of GA184.

These comparisons provide a relative overview of mitochondrial ROS generation in selected strains, which was a main objective of this study. The results showed compelling evidence supporting the notion that the majority of the strains had significant variations in ROS levels in comparison to the wild type. These differences also confirmed inherent biological variations, genetic differences or environmental influences impacting ROS regulation in these strains. In addition, all the strains treated with rotenone showed a significant increase in ROS levels, which indicated good control. This further showed that the OXPHOS system is under stress and extra stress. Rotenone had a big impact on the ROS levels. The increased ROS in some mutants relates to what was expected, because a dysfunction of any gene in the OXPHOS can lead to increased ROS. The mutants that have increased ROS reflected compromised mitochondrial health, resulting in high ROS levels.

CHAPTER 5 SUMMARY AND CONCLUSION

5.1 INTRODUCTION

This study highlighted and addressed a limitation in the *in vitro* investigations of mitochondrial disease models, specifically the lack of well-characterized mitochondrial ROS production in *in vivo* studies where interventions of redox modulation or antioxidants are tested. An example of this is the well-known and frequently used complex I (NDUFS4) knockout model in mice, which resembles the phenotype of one of the most common mitochondrial diseases, called Leigh syndrome (Kruse *et al*, 2008). In recent studies where redox interventions were attempted on this model, including metallothioneins, it was apparent that a limitation of this disease model is the absence of a clear demonstration of ROS production and markers of oxidative stress (Miller *et al*, 2021).

5.2 SUMMARY

Thus, the problem that was identified in this study is the lack of a well-characterized *in vivo* model of primary OXPHOS deficiency that displays elevated mitochondrial ROS production, which could provide better defined options for future redox intervention studies. For this, the well characterized and widely used *C. elegans* was selected as base organism.

The aim of this study was the evaluation of ROS production in a selected number of OXPHOS knockout strains of *C. elegans*. To reach this aim, the following five objectives were identified with experimental strategies to achieve these objectives:

1. Identify from literature the available OXPHOS-deficient *C. elegans* strains and controls;

2. Acquisition of selected strains and establish general procedures for culturing and maintaining of *C. elegans*;

3. Confirm the genetic knockout in the selected strains using molecular genotyping analysis;

4. Biochemical characterization of selected strains using respiration, behavioural and other phenotypical characteristics;

5. ROS measurement of mitochondrial- and total ROS in the selected strains.

For the first two objectives, a thorough evaluation of the literature was conducted, resulting in the identification of five *C. elegans* strains with a pathogenic genetic variant in genes of any of the five OXPHOS complexes (see Table 3.1): three for complex I (MQ1333, CW152 and LB25), one for complex II (TK22) and one for complex III (MQ887). In addition, when the strains were obtained, the wild type N2 strain as well as a putative ROS forming SOD knockout strain (GA184) were obtained. After obtaining these strains, and as *C. elegans* as a research model was not yet established in the laboratory where this study was conducted, the methods for handling and maintaining these animals had to be developed.

The third objective was to confirm the genotypes of these strains. Genetic confirmation was important as there was no phenotypic characteristic that could be used to confirm the identity of the acquired strains. This was successfully done using genetic information on these strains and applying PCR and Sanger sequencing of the amplified regions where the variants were present. Comparing the data to the wild-type information, the variants in all the strains were confirmed, giving confidence that identities of the strains were correct and that functional investigations could continue. The fourth objective was to characterize and confirm the effect of the various variants on OXPHOS function. This was done using high resolution respirometry and effect on muscle function via locomotion analysis. For all the strains, to variable degrees, a reduction of respiration and locomotion were observed.

The key objective of this study was the comparative analysis of mitochondrial superoxide (ROS) in these various strains. This was done using a very specific area (pharyngeal bulb) of the nematode that allowed a more accurate estimation of mitochondrial ROS compared to other less specific techniques. As with the other functional investigations, ROS production also varied among the strains, as expected, but a clear indication could be made of which strains generated the most ROS, thus reaching the aim of this study.

To compare the key results of this study, Figure 5.1 provides a comparison of the three functional investigations of the strains, to be able to make final conclusions. This figure only compares the order of most affected strains in the three parameters, and not an accurate scale of the differences.

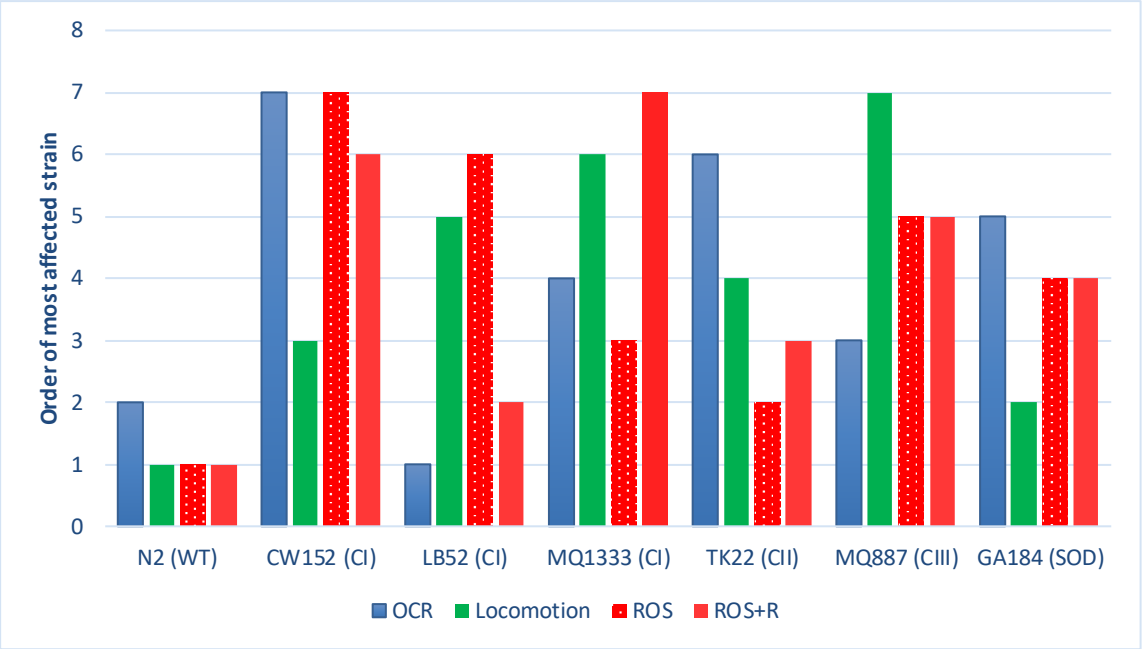

Figure 5.1. Comparison of relevant functional parameters between strains. The figure lists the strains used and relative order in which the strains were affected (1 being the least and 7 the most) during the evaluation of oxygen consumption rate (OCR), locomotion and production of mitochondrial superoxide without (ROS) and with rotenone (ROS+R). Strains are grouped according to proteins affected (CI, CII, CIII and SOD).

Considering this comparison, most of the strains were affected by their variants and showed great significance in increased ROS. Firstly, the strains that showed the highest increased ROS were; CW152, LB25 and MQ887 KO, and these were significantly affected ($P<0.05$) for the three parameters (OCR, ROS and locomotion), compared to the wild-type. Secondly, GA184 emerges as a promising candidate for future ROS-related studies and as a reliable control reference in comparison to the wild-type strain, exhibiting sufficient distinctions warranting its utilization. Thirdly, MQ887, MQ1333 and LB25 were significantly affected during locomotion analyses. Lastly, TK22 strain would be useful for oxygen consumption and locomotion analyses. Additionally, the wild-type treated with rotenone also shows significant differences in all the analyses, indicating a good reliable control to use during OXPHOS related studies. Taking all the analyses together, for future ROS related studies, the most suitable strains would be CW152, LB25, MQ887 and MQ1333.

5.3 GENERAL SIGNIFICANCE

The study of molecular mechanisms underlying the alterations in mitochondrial functionality can be extremely relevant for the understanding of mitochondrial disorders. In this study *C. elegans* confirmed that it could be a useful *in vivo* model for studying key pathophysiological features of OXPHOS dysfunction, such as ROS. Notably, *C. elegans* as a simple and pluricellular organism could open interesting perspectives to better investigate the pathophysiological mechanisms underlying the devastating diseases associated with OXPHOS dysfunction. Due to its fast life cycle, ease of handling and modifying, it may be particularly suitable as an *in vivo* platform for multi-drug screening for developing novel therapeutic approaches.

Comparing the various OXPHOS knockout models of CI, CII and CIII, the variability in the effect of the various variants/strains on the three key parameters was evident. When examining these knockout models individually, each displays distinct characteristics and responses, which is not unexpected for mitochondrial disease models of various kinds. This can be found throughout literature. In a study by Lapuente-Brun *et al*. (2013) using CI-deficient mouse models, it was observed that CI dysfunction leads to neurodegenerative phenotypes resembling Leigh syndrome. These mice displayed various neurological and muscle impairments due to the deficiency in energy production. A study by Liu *et al*. (2020) investigated CII-deficient models in *C elegans*, which highlighted that while CII-deficient mutants exhibited impaired mitochondrial respiration, they also showed altered metabolic profiles affecting various cellular processes such as mitochondrial dysfunction and cellular senescence. Similarly, for CIII-deficiency in mice, the deficiency led to a spectrum of mitochondrial disorders with varying phenotypic presentations, showcasing the critical role of CIII in maintaining cellular energy homeostasis (Fernandez-Vizarra *et al*., 2010).

In this study, the comprehensive analyses on confirmed genotypes associated with mitochondrial disease, of mitochondrial function/respiration and ROS levels in different strains, and the variability that it showed – which is a hallmark of the disease - provides a bases for further investigations, beyond the scope of this study, on the interactions of these and other cell biological responses that are involved in the pathophysiology of mitochondrial disorders. The confirmation of identified variations and genotypes for downstream analysis lays a crucial foundation for understanding the specific genetic components influencing mitochondrial function. Notably, the *C. elegans* mutants exhibiting decreased oxygen consumption rates align with the anticipated outcomes, affirming that the KO associated with OXPHOS will likely impede mitochondrial function. The correlation underscores the pivotal role these genes play and that they may contribute to an increase in mitochondrial ROS and affecting the mitochondria in general.

The significant variation in ROS levels, oxygen consumption and movement among certain strains compared to the wild-type, offers compelling evidence of the impact of these mutations on cellular oxidative stress. Moreover, the observed differences in locomotor behaviour between wild-type worms and certain mutated strains, wherein mutants exhibit a shorter duration of forward movement before reversing and altering direction, adds another layer of multifaceted impact of these genetic variations. The behavioural disparity underscores the broader physiological implications of these mutants beyond cellular respirations, potentially implicating neuronal function, or muscular control, both of which could be intertwined with the observed alterations in mitochondrial function and ROS levels. Continued advancements in genetic manipulation techniques, imaging technologies, and omics approaches will further enhance our understanding of mitochondrial dysfunction. Moreover, the ability to perform large-scale screens and the potential for personalized medicine based on genetic variations in *C. elegans* offer promising avenues for targeted interventions.

Ultimately, these findings collectively emphasize the intricate interplay between genetic variants, mitochondrial function, oxidative stress, and ROS. Understanding these connections not only contributes to knowledge in *C. elegans*' ROS and cellular respiration that may help for therapeutic interventions, but also potential avenues for targeted treatments also aimed at mitigating the adverse effects of mitochondrial dysfunction and ROS. Furthermore, after confirming these KO and that ROS influences these nematodes can be further used in hypothesis generating and -testing studies. Further exploration into the specific mechanisms underlying these observed effects could unveil novel therapeutic targets and strategies for addressing a spectrum of conditions linked to mitochondrial dysfunction, ROS and oxidative stress.

BIBLIOGRAPHY

Alberts, B., Johnson, A., Lewis, J., Raff, M., Roberts, K. & Walter, P., 2002. Integrins. In Molecular Biology of the Cell. 4th edition. Garland Science. 2002. Electron-Transport Chains and Their Proton Pumps. Molecular Biology of the Cell., https://www.ncbi.nlm.nih.gov/books/NBK26904/.

Anderson, E.N., Corkins, M.E., Li, J.-C., Singh, K., Parsons, S., Tucey, T.M. & Sinclair, D.A. 2016. *C. elegans* lifespan extension by osmotic stress requires FUdR, base excision repair, FOXO, and sirtuins. Mechanisms of ageing and development, 154:30-42.

Back, P., Braeckman, B.P. & Matthijssens, F. 2012. ROS in aging Caenorhabditis elegans: damage or signaling? Oxidative Medicine and Cellular Longevity, 2012:608478. https://www.ncbi.nlm.nih.gov/pubmed/22966416 10.1155/2012/608478.

Balaban, R.S., Nemoto, S. & Finkel, T. 2005. Mitochondria, oxidants, and aging. Cell, 120(4):483-495.

Bansal, S., Srinivasan, S., Anandasadagopan, S., Chowdhury, A. R., Selvaraj, V., Kalyanaraman, B., Joseph, J., & Avadhani, N. G. 2012. Additive effects of mitochondrion-targeted cytochrome CYP2E1 and alcohol toxicity on cytochrome c oxidase function and stability of respirosome complexes. The Journal of biological chemistry, 287:15284-15297. https://doi.org/10.1074/jbc.M111.314062.

Halliwell, B. 1991. Drug Antioxidant Effects. Drugs 42, 569–605. https://doi.org/10.2165/00003495-199142040-00003.

Bass, D., Parce, J.W., Dechatelet, L.R., Szejda, P., Seeds, M. & Thomas, M. 1983. Flow cytometric studies of oxidative product formation by neutrophils: a graded response to membrane stimulation. The Journal of Immunology, 130(4):1910-1917.

Brenner, S. 1974. The genetics of Caenorhabditis elegans..pdf. Genetics, 77(1):71-94.

Brenner, S. 1988. The nematode Caenorhabditis elegans. Cold Spring Harbor Laboratory 1, 988.

Burnell, A.M., Houthoofd, K., O'Hanlon, K. & Vanfleteren, J.R., 2005. Alternate metabolism during the dauer stage of the nematode Caenorhabditis elegans. Experimental gerontology, 40(11), pp.850-856.

Chinnery, P.F. 2014. Mitochondrial disorders overview. In. GeneReviews®: University of Washington, Seattle. https://www.ncbi.nlm.nih.gov/books/NBK1224/.

Chinnery, P.F. & Schon, E.A. 2003. Mitochondria. Journal of Neurology, Neurosurgery & Psychiatry, 74(9):1188-1199.

Cohen, B.H. 2019. Mitochondrial and metabolic myopathies. Continuum: Lifelong Learning in Neurology, 25(6):1732-1766.

Colman, R.J., Beasley, T.M., Kemnitz, J.W., Johnson, S.C., Weindruch, R. & Anderson, R.M. 2014. Caloric restriction reduces age-related and all-cause mortality in rhesus monkeys. Nature communications, 5(1):1-5.

Cooke, M.S., Evans, M.D., Dizdaroglu, M. & Lunec, J.J.T.F.J. 2003. Oxidative DNA damage: mechanisms, mutation, and disease. 17(10):1195-1214.

Cooper, G.M., Hausman, R.E. & Hausman, R.E. 2007. The cell: a molecular approach. 4th edition. American Society for Microbiology. Washington, DC.

Corsi, A.K. 2006. A Biochemist's Guide to *C. elegans*. Analytical Biochemistry, 359(1):1–17.

Corsi, A.K., Wightman, B. & Chalfie, M. 2015. A Transparent window into biology: A primer on Caenorhabditis elegans. WormBook:1-31. https://www.ncbi.nlm.nih.gov/pubmed/26087236 10.1895/wormbook.1.177.1.

Denzel, M.S., Lapierre, L.R. & Mack, H.I., 2019. Emerging topics in C. elegans aging research: Transcriptional regulation, stress response and epigenetics. Mechanisms of ageing and development, 177, pp.4-21.

Devasagayam, T.P., Tilak, J. C., Boloor, K. K., Sane, K. S., Ghaskadbi, S. S., & Lele, R. D. .2004. Free radicals and antioxidants in human health: current status and future prospects. The Journal of the Association of Physicians of India, 52:794-804.

Doerrier, C., Garcia-Souza, L.F., Krumschnabel, G., Wohlfarter, Y., Mészáros, A.T. & Gnaiger, E., 2018. High-resolution FluoRespirometry and OXPHOS protocols for human cells, permeabilized fibers from small biopsies of muscle, and isolated mitochondria. Mitochondrial Bioenergetics: Methods and Protocols, pp.31-70.

Dilberger, B., Baumanns, S., Schmitt, F., Schmiedl, T., Hardt, M., Wenzel, U. & Eckert, G.P. 2019. Mitochondrial Oxidative Stress Impairs Energy Metabolism and Reduces Stress Resistance and

Longevity of *C. elegans*. Oxid Med Cell Longev, 2019:6840540. https://www.ncbi.nlm.nih.gov/pubmed/31827694 10.1155/2019/6840540.

DiMauro, S. & Andreu, A.L. 2000. Mutations in mtDNA: are we scraping the bottom of the barrel? Brain Pathology, 10(3):431-441.

DiMauro, S. & Schon, E.A. 2003. Mitochondrial respiratory-chain diseases. New England Journal of Medicine, 348(26):2656-2668.

DiMauro, S., Schon, E.A., Carelli, V. & Hirano, M. 2013. The clinical maze of mitochondrial neurology. Nature Reviews Neurology, 9(8):429-444.

Dingley, S., Polyak, E., Lightfoot, R., Ostrovsky, J., Rao, M., Greco, T. & Falk, M.J. 2010. Mitochondrial respiratory chain dysfunction variably increases oxidant stress in Caenorhabditis elegans. Mitochondrion, 10(2):125-136. https://www.ncbi.nlm.nih.gov/pubmed/19900588 10.1016/j.mito.2009.11.003.

Distelmaier, F., Koopman, W.J., van den Heuvel, L.P., Rodenburg, R.J., Mayatepek, E., Willems, P.H. & Smeitink, J.A. 2009. Mitochondrial complex I deficiency: from organelle dysfunction to clinical disease. Brain, 132(4):833-842.

Duchen, M.R. 2004. Mitochondria in health and disease: perspectives on a new mitochondrial biology. Molecular aspects of medicine, 25(4):365-451.

Dudkina, N.V., Kouřil, R., Peters, K., Braun, H.P. & Boekema, E.J., 2010. Structure and function of mitochondrial supercomplexes. Biochimica et Biophysica Acta (BBA)-Bioenergetics, 1797(6-7), pp.664-670.

Dues, D.J., Andrews, E.K., Schaar, C.E., Bergsma, A.L., Senchuk, M.M. & Van Raamsdonk, J.M. 2016. Aging causes decreased resistance to multiple stresses and a failure to activate specific stress response pathways. Aging (Albany NY), 8(4):777.

Ebadi, M. 2001. Antioxidants and free radicals in health and disease: An introduction to reactive oxygen species, oxidative injury, neuronal cell death and therapy in neurodegenerative diseases. Crit. Rev. Toxicology, 38:13-71.

Falk, M.J., Zhang, Z., Rosenjack, J.R., Nissim, I., Daikhin, E., Sedensky, M.M., Yudkoff, M. & Morgan, P.G., 2008. Metabolic pathway profiling of mitochondrial respiratory chain mutants in C. elegans. Molecular genetics and metabolism, 93(4), pp.388-397.

Fay, D.S. 2013. Classical genetic methods. WormBook: the online review of *C. elegans* biology.1-58. 10.1895/wormbook.1.165.1.

Gao, A.W., uit de Bos, J., Sterken, M.G., Kammenga, J.E., Smith, R.L. & Houtkooper, R.H., 2018. Forward and reverse genetics approaches to uncover metabolic aging pathways in Caenorhabditis elegans. Biochimica et Biophysica Acta (BBA)-Molecular Basis of Disease, 1864(9), pp.2697-2706.

Gorman. G.S., Schaefer, A.M., Ng, Y., Gomez N., Blakely E.L., Alston C.L., Feeney C., Horvath R., Yu-Wai-Man P., Chinnery P.F. & Taylor RW. 2015. Prevalence of nuclear and mitochondrial DNA mutations related to adult mitochondrial disease. Annals of neurology. 77(5):753-9.

Gorman, G.S., Chinnery, P.F., DiMauro, S., Hirano, M., Koga, Y., McFarland, R. & Turnbull, D.M. 2016. Mitochondrial diseases. Nature reviews Disease primers, 2(1):1-22.

Grad, L.I. & Lemire, B.D., 2004. Mitochondrial complex I mutations in Caenorhabditis elegans produce cytochrome c oxidase deficiency, oxidative stress and vitamin-responsive lactic acidosis. Human molecular genetics, 13(3), pp.303-314.

Gray, J. & Lissmann, H. 1964. The locomotion of nematodes. Journal of Experimental Biology, 41(1):135-154.

Gropman, A.L. 2004. The neurological presentations of childhood and adult mitochondrial disease: established syndromes and phenotypic variations. Mitochondrion, 4(5-6):503-520.

Gruber, J., Chen, C.-B., Fong, S., Ng, L.F., Teo, E. & Halliwell, B. 2015. Caenorhabditis elegans: what we can and cannot learn from aging worms. Antioxidants and redox signaling, 23(3):256-279.

Haas, R.H., Parikh, S., Falk, M.J., Saneto, R.P., Wolf, N.I., Darin, N. & Cohen, B.H. 2007. Mitochondrial disease: a practical approach for primary care physicians. Pediatrics, 120(6):1326-1333.

Halliwell, B. & Gutteridge, J.M. 2015. Free radicals in biology and medicine. Oxford university press, USA.

Haspel, G. & O'Donovan, M.J. 2011. A perimotor framework reveals functional segmentation in the motoneuronal network controlling locomotion in Caenorhabditis elegans. Journal of Neuroscience, 31(41):14611-14623.

Hench, J., Bratić Hench, I., Pujol, C., Ipsen, S., Brodesser, S., Mourier, A., Trifunović, A. 2011. A tissue-specific approach to the analysis of metabolic changes in Caenorhabditis elegans. PLoS One, 6(12):e28417.

Hicks, K.A., Howe, D.K., Leung, A., Denver, D.R. & Estes, S. 2012. In vivo quantification reveals extensive natural variation in mitochondrial form and function in Caenorhabditis briggsae.

Holmgren, A., Johansson, C., Berndt, C., Lönn, M., Hudemann, C. & Lillig, C. 2005. Thiol redox control via thioredoxin and glutaredoxin systems. Biochemical Society Transactions, 33(6):1375-1377.

Hu, Q., D'Amora, D.R., MacNeil, L.T., Walhout, A.J. and Kubiseski, T.J., 2018. The Caenorhabditis elegans oxidative stress response requires the NHR-49 transcription factor. G3: Genes, Genomes, Genetics, 8(12), pp.3857-3863.Johnston, A.D. & Ebert, P.R. 2012. The redox system in *C. elegans*, a phylogenetic approach. Journal of toxicology, 2012.

Keston, A.S. & Brandt, R. 1965. The fluorometric analysis of ultramicro quantities of hydrogen peroxide. Analytical biochemistry, 11(1):1-5.

Knoefler, D. 2012. The role of hydrogen peroxide in the lifespan of Caenorhabditis elegans. (Thesis – PhD).

Koopman, M., Michels, H., Dancy, B.M., Kamble, R., Mouchiroud, L., Auwerx, J., Nollen, E.A. & Houtkooper, R.H., 2016. A screening-based platform for the assessment of cellular respiration in Caenorhabditis elegans. Nature protocols, 11(10):1798-1816.

Kruse, S.E., Watt, W.C., Marcinek, D.J., Kapur, R.P., Schenkman, K.A. & Palmiter, R.D. 2008. Mice with mitochondrial complex I deficiency develop a fatal encephalomyopathy. Cell Metabolism, 7(4):312-320.

Kwok, T.C., Ricker, N., Fraser, R., Chan, A.W., Burns, A., Stanley, E.F., ... Roy, P.J. 2006. A small-molecule screen in *C. elegans* yields a new calcium channel antagonist. Nature, 441(7089):91-95.

Lapuente-Brun, E., Moreno-Loshuertos, R., Acín-Pérez, R., Latorre-Pellicer, A., Colás, C., Balsa, E., Perales-Clemente, E., Quirós, P.M., Calvo, E., Rodríguez-Hernández, M.A. & Navas, P., 2013.

Supercomplex assembly determines electron flux in the mitochondrial electron transport chain. Science, 340(6140), pp.1567-1570.

Leung, M.C., Williams, P.L., Benedetto, A., Au, C., Helmcke, K.J., Aschner, M. & Meyer, J.N. 2008. Caenorhabditis elegans: an emerging model in biomedical and environmental toxicology. Toxicol Sci, 106(1):5-28. https://www.ncbi.nlm.nih.gov/pubmed/18566021 10.1093/toxsci/kfn121.

Lindeque, J.Z., Levanets, O., Louw, R. & van der Westhuizen, F.H. 2010. The involvement of metallothioneins in mitochondrial function & disease. Current Protein and Peptide Science, 11(4):292 - 309. 10.2174/138920310791233378.

Liping C., L.M., Qing B., Xiaonian Z., Jinmiao Z., Qing W., Daochuan L., Chen G., Jie L., Zhengbao Z., Caixia L., Zhini H., Xiaowen Z., Aihua Z., Weidong Q., Zhixiong Z., Wen C., and Yongmei Xiao. 2014. Heavy Metal-induced Metallothionein Expression Is Regulated by Specific Protein Phosphatase 2A Complexes. THE JOURNAL OF BIOLOGICAL CHEMISTRY, 289:22413–22426. 10.1074/jbc.M114.548677.

Liu, Y.J., McIntyre, R.L., Janssens, G.E., Williams, E.G., Lan, J., van Weeghel, M., Schomakers, B., van der Veen, H., van der Wel, N.N., Yao, P. & Mair, W.B., 2020. Mitochondrial translation and dynamics synergistically extend lifespan in *C. elegans* through HLH-30. Journal of Cell Biology, 219(6).

Lodish, H., Berk, A., Matsudaira, P., Kaiser, C.A., Krieger, M. & Scott, M.P. 2005 Molecular cell biology. 5th Edition, W.H. Freeman and Co., New York.

Luz, A.L., Rooney, J.P., Kubik, L.L., Gonzalez, C.P., Song, D.H. & Meyer, J.N., 2015. Mitochondrial morphology and fundamental parameters of the mitochondrial respiratory chain are altered in Caenorhabditis elegans strains deficient in mitochondrial dynamics and homeostasis processes. PloS one, 10(6), p.e0130940.

Machiela, E., Dues, D.J., Senchuk, M.M. & Van Raamsdonk, J.M. 2016. Oxidative stress is increased in *C. elegans* models of Huntington's disease but does not contribute to polyglutamine toxicity phenotypes. Neurobiology Dis, 96:1-11. https://www.ncbi.nlm.nih.gov/pubmed/27544481 10.1016/j.nbd.2016.08.008.

Maglioni, S. & Ventura, N. 2016. *C. elegans* as a model organism for human mitochondrial associated disorders. Mitochondrion, 30:117-125. https://www.ncbi.nlm.nih.gov/pubmed/26906059 10.1016/j.mito.2016.02.003.

Maglioni, S., Schiavi, A., Melcher, M., Brinkmann, V., Luo, Z., Raimundo, N., Laromaine, A., Meyer, J., Distelmaier, F. & Ventura, N. 2020. Lutein restores synaptic functionality in a *C. elegans* model for mitochondrial complex I deficiency. bioRxiv, https://doi.org/10.1101/2020.02.20.957225.

Mattiazzi, M., Vijayvergiya, C., Gajewski, C.D., DeVivo, D.C., Lenaz, G., Wiedmann, M. & Manfredi, G. 2004. The mtDNA T8993G (NARP) mutation results in an impairment of oxidative phosphorylation that can be improved by antioxidants. Human molecular genetics, 13(8):869-879.

McCord, J.M., Keele, B. B., Jr, & Fridovich, I. 1971. An enzyme-based theory of obligate anaerobiosis: the physiological function of superoxide dismutase. Proceedings of the National Academy of Sciences of the United States of America, 68:1024-1027. https://doi.org/10.1073/pnas.68.5.1024.

McFarland, R., Taylor, R.W. & Turnbull, D.M. 2010. A neurological perspective on mitochondrial disease. The Lancet Neurology, 9(8):829-840.

Miller, H.C. 2020. Investigation into the protection of mitochondrial disease pathology by metallothionein overexpression. (Thesis – PhD).

Miller, H.C., Louw, R., Mereis, M., Venter, G., Boshoff, J.D., Mienie, L., Van Reenen, M., Venter, M., Lindeque, J.Z., Domínguez-Martínez, A. & Quintana, A. 2021. Metallothionein 1 overexpression does not protect against mitochondrial disease pathology in Ndufs4 knockout mice. Molecular Neurobiology, 58(1) pp.243-262.

Miquel, J., Economos, A., Fleming, J. & Johnson Jr, J. 1980. Mitochondrial role in cell aging. Experimental gerontology, 15(6):575-591.

Miranda-Vizuete, A. & Veal, E.A. 2017. Caenorhabditis elegans as a model for understanding ROS function in physiology and disease. Redox Biology, 11:708-714. https://www.ncbi.nlm.nih.gov/pubmed/28193593 10.1016/j.redox.2016.12.020.

Miwa, S., Kashyap, S., Chini, E. & von Zglinicki, T. 2022. Mitochondrial dysfunction in cell senescence and aging. Journal of Clinical Investigation, 132(13):e158447.

Mrityunjaya, M., Pavithra, V., Neelam, R., Janhavi, P., Halami, P. & Ravindra, P. 2020. Immune-boosting, antioxidant and anti-inflammatory food supplements targeting pathogenesis of COVID-19. Frontiers in immunology:2337.

Murrant, C.L., & Reid, M. B. 2001. Detection of reactive oxygen and reactive nitrogen species in skeletal muscle. Microscopy research and technique, 55:236-248.

Niki, E. 1987. Antioxidants in relation to lipid peroxidation. Chemistry and physics of lipids, 44(2-4):227-253.

Niyazov, D.M., Kahler, S.G. & Frye, R.E. 2016. Primary mitochondrial disease and secondary mitochondrial dysfunction: importance of distinction for diagnosis and treatment. Molecular syndromology, 7(3):122-137.

Obre, E. & Rossignol, R. 2015. Emerging concepts in bioenergetics and cancer research: metabolic flexibility, coupling, symbiosis, switch, oxidative tumors, metabolic remodelling, signalling and bioenergetic therapy. The international journal of biochemistry and cell biology, 59:167-181.

Radi, R., Beckman, J.S., Bush, K.M. & Freeman, B.A. 1991. Peroxynitrite-induced membrane lipid peroxidation: the cytotoxic potential of superoxide and nitric oxide. Archives of biochemistry and biophysics, 288(2):481-487.

Reinecke, F., Smeitink, J.A. & Van Der Westhuizen, F.H. 2009. OXPHOS gene expression and control in mitochondrial disorders. Biochimica et Biophysica Acta (BBA)-Molecular Basis of Disease, 1792(12):1113-1121.

Reinecke, F., Levanets, O., Olivier, Y., Louw, R., Semete, R., Grobler, A., Hidalgo, J., Smeitink, J., Olckers, A. & Van der Westhuizen, F.H. 2006. Metallothionein isoform 2A expression is inducible and protects against ROS-mediated cell death in rotenone-treated HeLa cells. Biochemical Journal, 395:405-415.

Riddle, D.L., Blumenthal T., Meyer B.J., & Priess J.R. 1997. C. elegans II. 2nd edition. Cold Spring Harbor (NY): Cold Spring Harbor Laboratory Press; 1997. Available from: https://www.ncbi.nlm.nih.gov/books/NBK19997/

Ruzzenente, B., Rötig, A. & Metodiev, M.D. 2016. Mouse models for mitochondrial diseases. Human Molecular Genetics, 25(R2):pp.R115-R122.

Schaar, C.E., Dues, D.J., Spielbauer, K.K., Machiela, E., Cooper, J.F., Senchuk, M., Hekimi, S. & Van Raamsdonk, J.M. 2015. Mitochondrial and cytoplasmic ROS have opposing effects on lifespan. PLoS genet, 11:e1004972.

Schafer, F.Q. & Buettner, G.R. 2001. Redox environment of the cell as viewed through the redox state of the glutathione disulfide/glutathione couple. Free radical biology and medicine, 30(11):1191-1212.

Schindelin, J., Arganda-Carreras, I., Frise, E., Kaynig, V., Longair, M., Pietzsch, T. & Schmid, B. 2012. Fiji: an open-source platform for biological-image analysis. Nature methods, 9(7):676-682.

Seddon, I. 2016. Quantifying the locomotion of *C. elegans* and their response to photo stimulation. https://scholarship.rollins.edu/honors/41.

Senoo-Matsuda, N., Hartman, P.S., Akatsuka, A., Yoshimura, S. & Ishii, N. 2003. A complex II defect affects mitochondrial structure, leading to ced-3-and ced-4-dependent apoptosis and aging. Journal of Biological Chemistry, 278(24):22031-22036.

Senoo-Matsuda, N., Yasuda, K., Tsuda, M., Ohkubo, T., Yoshimura, S., Nakazawa, H. & Ishii, N. 2001. A defect in the cytochrome b large subunit in complex II causes both superoxide anion overproduction and abnormal energy metabolism in Caenorhabditis elegans. 276(45):41553-41558.

Sharma, M., Pandey, R. & Saluja, D. 2018. ROS is the major player in regulating altered autophagy and lifespan in sin-3 mutants of *C. elegans*. Autophagy, 14(7):1239-1255. https://www.ncbi.nlm.nih.gov/pubmed/29912629 10.1080/15548627.2018.1474312.

Siekevitz, P. 1957. Powerhouse of the Cell. Scientific American, 197(1):131-144. https://www.jstor.org/stable/10.2307/24940890.

Stiernagle, T. 1999. Maintenance of *C. elegans*. *C. elegans*, 2:51-67.

Taferner, A., Pircher, H., Koziel, R., von Grafenstein, S., Baraldo, G., Palikaras, K. & Jansen-Dürr, P. 2015. FAH domain containing protein 1 (FAHD-1) is required for mitochondrial function and locomotion activity in *C. elegans*. PLoS One, 10(8):e0134161.

Tan, S., Schubert, D. & Maher, P. 2001. Oxytosis: a novel form of programmed cell death. Current topics in medicinal chemistry, 1:497-506.

Thannickal, V.J. & Fanburg, B.L. 2000. Reactive oxygen species in cell signaling. 279(6):1005-1028. https://journals.physiology.org/doi/abs/10.1152/ajplung.2000.279.6.L1005 10.1152/ajplung.2000.279.6.L1005.

Tiet, M.Y., Lin, Z., Gao, F., Jennings, M.J. & Horvath, R. 2021. Targeted therapies for Leigh syndrome: systematic review and steps towards a 'Treatabolome'. Journal of neuromuscular diseases, 8(6):885-897.

Turrens, J.F. 1997. Superoxide production by the mitochondrial respiratory chain. Bioscience reports, 17:3-8.

Tzameli, I. 2012. The evolving role of mitochondria in metabolism. Trends in Endocrinology and Metabolism, 23(9):417-419.

Van Breusegem, F., Slooten, L., Stassart, J.-M., Botterman, J., Moens, T., Van Montagu, M. & Inzé, D. 1999. Effects of overproduction of tobacco MnSOD in maize chloroplasts on foliar tolerance to cold and oxidative stress. Journal of Experimental Botany, 50(330):71-78.

Van Raamsdonk, J.M., Meng, Y., Camp, D., Yang, W., Jia, X., Bénard, C. & Hekimi, S. 2010. Decreased energy metabolism extends life span in Caenorhabditis elegans without reducing oxidative damage. Genetics, 185(2):559-571.

Van Raamsdonk, J.M. & Hekimi, S., 2010. Reactive oxygen species and aging in Caenorhabditis elegans: causal or casual relationship?. Antioxidants & redox signaling, 13(12), pp.1911-1953.

Vanfleteren, J.R. 1993. Oxidative stress & ageing in Caenorhabditis elegans. Biochemical Journal, 292(2):605-608.

Vašák, M. 2005. Advances in metallothionein structure & functions. Journal of Trace Elements in Medicine & Biology, 19(1):13-17.

Ventura, N., Rea, S.L. & Testi, R. 2006. Long-lived *C. elegans* mitochondrial mutants as a model for human mitochondrial-associated diseases. Exp Gerontol, 41(10):974-991. https://www.ncbi.nlm.nih.gov/pubmed/16945497 10.1016/j.exger.2006.06.060.

Weydert, C.J., & Cullen, J. J. 2010. Measurement of superoxide dismutase, catalase & glutathione peroxidase in cultured cells & tissue. Nature protocols, 5:51-66. https://doi.org/10.1038/nprot.2009.197.

WormBase. 2022. WormBase Overview. https://wormbase.org/#012-34-5 Date of access: 20 Jun. 2022.

Xiao, H., Xie, Y., Xi, K., Xie, J., Liu, M., Zhang, Y., Cheng, Z., Wang, W., Guo, B. & Wu, S., 2023. Targeting mitochondrial sirtuins in age-related neurodegenerative diseases and fibrosis. Aging and Disease, 14(5), p.1583.

Xu, T., Ding, W., Ji, X., Ao, X., Liu, Y., Yu, W. & Wang, J., 2019. Oxidative stress in cell death & cardiovascular diseases. Oxidative medicine and cellular longevity, https://doi.org/10.1155/2019/9030563.

Yemini, E., Jucikas, T., Grundy, L.J., Brown, A.E. & Schafer, W.R. 2013. A database of Caenorhabditis elegans behavioral phenotypes. Nat Methods, 10(9):877-879. https://www.ncbi.nlm.nih.gov/pubmed/23852451 10.1038/nmeth.2560.

Zhang, T., Ni, C., Li, C., Lu, P., Chen, D., Dong, Y. & Xie, Z. 2021. Isoflurane impairs oogenesis through germ cell apoptosis in *C. elegans*. Scientific Reports, 11(1):14481.

Zhao, H., Joseph, J., Fales, H.M., Sokoloski, E.A., Levine, R.L., Vasquez-Vivar, J. & Kalyanaraman, B. 2005. Detection and characterization of the product of hydroethidine and intracellular superoxide by HPLC and limitations of fluorescence. Proceedings of the National Academy of Sciences, 102(16):5727-5732.

ANNEXURES

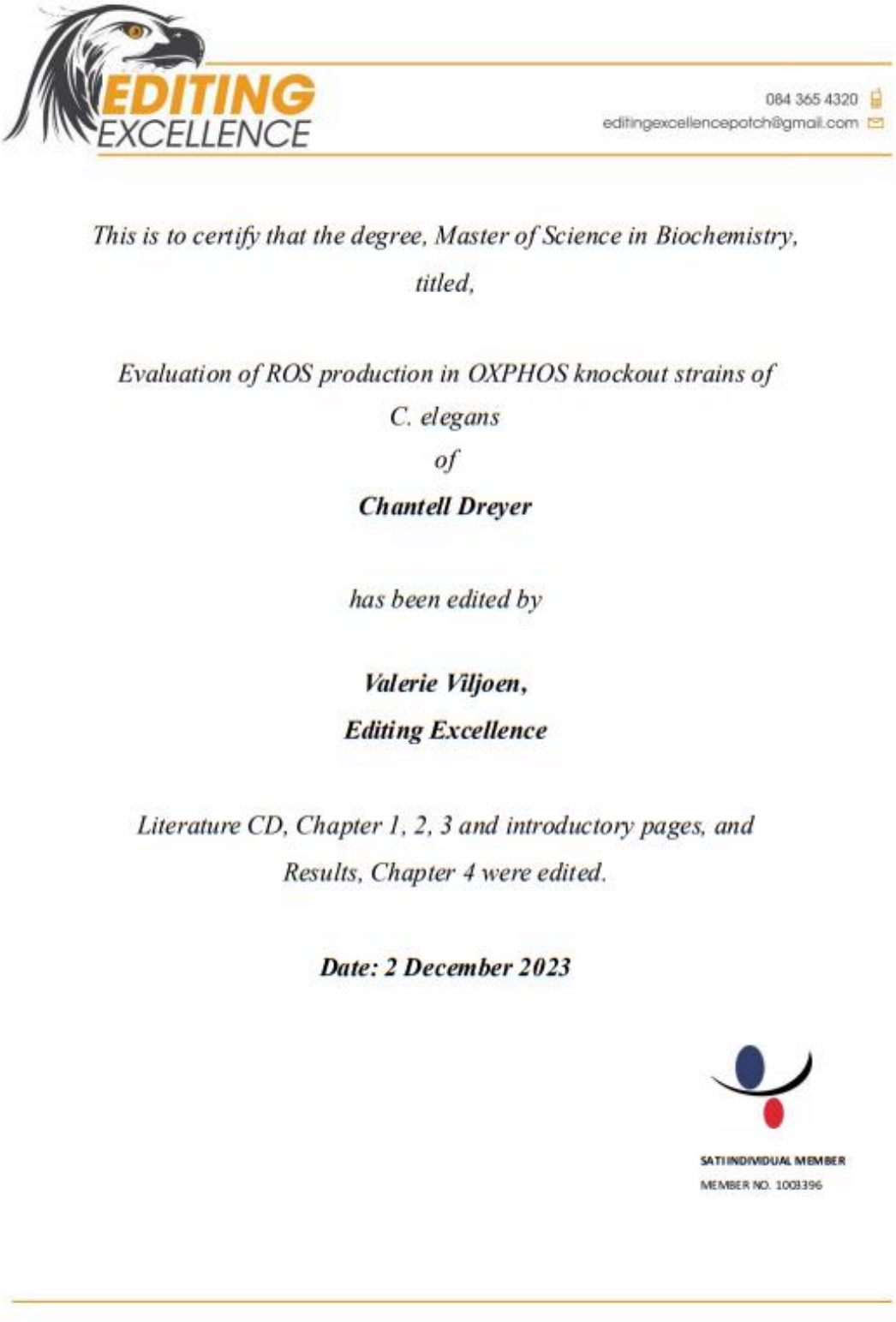

EDITING EXCELLENCE

084 365 4320
editingexcellencepotch@gmail.com

This is to certify that the degree, Master of Science in Biochemistry, titled,

Evaluation of ROS production in OXPHOS knockout strains of C. elegans

of

Chantell Dreyer

has been edited by

Valerie Viljoen,
Editing Excellence

Literature CD, Chapter 1, 2, 3 and introductory pages, and Results, Chapter 4 were edited.

Date: 2 December 2023

SATI INDIVIDUAL MEMBER
MEMBER NO. 1003396